eLife

Reviewed Preprint
v1 • June 3, 2024
Not revised

Cancer Biology

In vivo targeted and deterministic single cell malignant transformation

Pierluigi Scerbo, **Benjamin Tisserand**, **Marine Delagrange**, **Héloïse Debare**, **David Bensimon**, **Bertrand Ducos**

Laboratoire de Physique de l'Ecole Normale Supérieure LPENS, ENS, PSL Research University, CNRS, Sorbonne Université, Université de Paris, 24 rue Lhomond 75005 Paris, France • High Throughput qPCR Core Facility of the ENS, Ecole Normale Supérieure, PSL Research University, IBENS, 46 rue d'Ulm 75005 PARIS • Dept. Chemistry and Biochemistry, UCLA, 607 Young Dr.E, Los Angeles 90095

Abstract

Why does a normal cell possibly harboring genetic mutations in oncogene or tumor suppressor genes becomes malignant and develop a tumor is a subject of intense debate. Various theories have been proposed but their experimental test has been hampered by the unpredictable and improbable malignant transformation of single cells. Here using an optogenetic approach we permanently turn on an oncogene (KRASG12V) in a single cell of a zebrafish brain that, only in synergy with the transient co-activation of a reprogramming factor (VENTX/NANOG/OCT4), undergoes a deterministic malignant transition and robustly and reproducibly develops within 6 days into a full-blown tumor. The controlled way in which a single cell can thus be manipulated to give rise to cancer lends support to the "ground state theory of cancer initiation" through "short-range dispersal" of the first malignant cells preceding tumor growth.

eLife assessment

This study provides **valuable** initial characterization of a verterbrate embryonic system that demonstrates aspects of an optogenetically inducible hyperplasia model. Although the evidence provided is **incomplete** to conclude that the system is demonstrating tumor initiation from a single cell that is metastasizing that can be quantitatively assessed, the authors propose a mechanism whereby reactivation of re-programming factors correlates with the increased likelihood of a mutant cell undergoing malignant transformation. This work will be of interest to developmental and cancer biologists mainly for the novel genetic tools described.

https://doi.org/10.7554/eLife.97650.1.sa3

Introduction

How cancer arises from a single normal cell is still the subject of active debate, affecting intervention strategies. While many cells may harbor oncogenic mutations, only a few unpredictably end-up developing a full-blown tumor[1,2,3,4]. Various theories have been proposed to explain that transition[5,6,7,8], but none has been tested *in vivo* at the single cell level. Cancer initiation is thus believed to be a *rare* event taking place at the level of *individual cells*[9,10,11,12,13] arising as a result of the accumulation of genetic mutations in so called Mut-driver genes (oncogenes such as KRAS[14,15], tumor suppressor genes[16] such as TP53 or life-span[17] genes such as TERT). Notably, mutant KRAS is the most frequent driver of several cancers[18,19] : about 27% of all human cancers, 45% of colorectal and 90% of pancreatic cancers[20].

Recently, it has been shown that genes involved in embryonic development, pluri/multipotency and cell reprogramming such as VENTX/NANOG and POU5/OCT4 are abnormally reactivated in late cancer stages, where acting as Epigenetic Drivers (Epi-Drivers) they empower cancer cells with Cancer Stem Cell (CSCs) features, resistance to anti-cancer therapies and potential for cancer recurrence/relapse[21,22,23,24,25,26,27]. Although it is evident that such Epi-Drivers confer a selective advantage to CSCs in a full-blown cancer, whether they play a role during the early phases of malignant transformation is still unknown.

Current approaches to the study of cancer use constitutive or conditional expression of Mut-driver (or Epi-driver genes[28]) in specific tissues, i.e. in many cells, even though only a small subset of these cells eventually leads to the growth of tumors[29], often observed when the tumor already consists of many thousands of heterogeneous abnormal cells. Hence, carcinogenetic processes observed among sibling organisms[30,31,32] occur with variable latency period from the onset of induction, at different locations and develop asynchronously. As a result, the initial stages of tumorigenesis are difficult to study, the state of the cell(s) of origin difficult to assess and control while its cellular environment is perturbed by the induced expression of the Mut- or Epi-driver genes. Due to the rarity of the event *in vivo*[32], a statistically relevant single-cell tracking and characterization of the early stages of tumorigenesis has therefore never been done. This emphasises the need to predict or control the cell undergoing malignant transformation *in vivo* in order to pave the way for a study of the cellular and molecular events involved in the initial stages of tumorigenesis.

To address these issues, we have developed an optogenetic approach to control the expression of an oncogene in a single cell[33], with the goals of: (1) measuring the probability of the malignant transformation of a single cell in a live organism in various backgrounds and (2) tracking and characterising the development of a tumor from the original cell. **In the following we show that the synergy between only two factors: the oncogene kRasG12V and a reprogramming factor (Ventx, Nanog or Oct4) increases the probability of carcinogenesis from a single cell by many orders of magnitude when compared to the expression of either of these genes (or none)**.

Optogenetics approaches allow for the photocontrol and monitoring of the activity of biomolecules *in vivo*. The approach we developed uses a photoactivable analog of tamoxifen (caged cyclofen, cCYC) to control the activity of proteins fused to the ERT-receptor[34,35] (a modified estrogen binding domain[36]) (**Fig. 1A**). These protein constructs are sequestered by cytoplasmic chaperones. Once cCYC is uncaged by light (with one-photon illumination at ~375 nm or two-photon at ~750 nm), cyclofen (CYC) is released[34]. It binds to the ERT-receptor and releases the fused protein (e.g. a Cre-ERT recombinase) from its complex with cytoplasmic chaperones[35] (**Fig. 1A**).

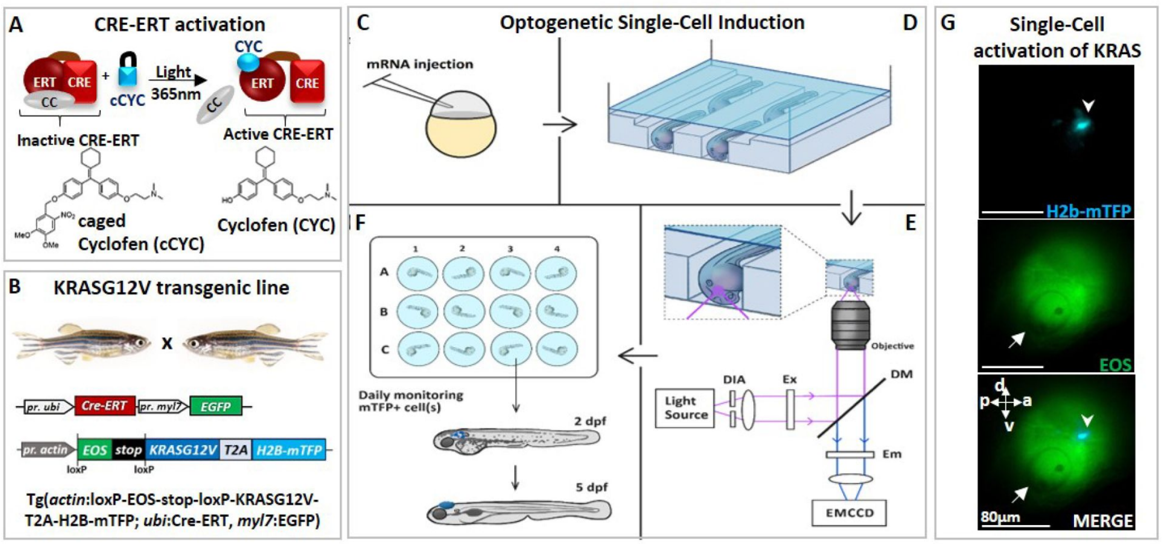

FIGURE 1

Optogenetic set-up for single cell induction.

(A) Photo-control of a protein fused to an Estrogen Receptor (ERT) is achieved by releasing the protein from its complex with cytoplasmic chaperones (CC), upon uncaging of cCYC. **(B)** The transgenic zebrafish line engineered to express an oncogene (KRASG12V) upon photo-activation of a CRE-recombinase fused to ERT (CRE-ERT) (as shown in A). **(C)** The mRNAs of Ventx-GR and mRFP (used as a marker) are injected at the one cell stage. **(D)** At 1dpf the embryos are mounted in channels in an agarose gel and incubated for 45 min in cCyc on a microscope stage. **(E)** They are washed and illuminated at 405nm on a microscope to uncage cCyc close to the otic vesicle. A diaphragm (DIA) defines an illumination zone of ~80µm diameter (see G). Excitation (EX), Dichroic mirrors (DM) and emission (EM) filters allow for visualization of Eos and mTFP. The cell in which KRASG12V has been induced is observed within ~1h by the fluorescence of mTFP (see G). **(F)** The embryos are transferred into individual wells, incubated overnight in DEX, washed at 1dpi and monitored over the next 5 days. **(G)** Lateral view of zebrafish at ~1h post-activation displays a single induced cell (top: blue spot shown by arrowhead in mTFP channel) in the illumination region (middle: Eos channel) in the vicinity of the otic vesicle (white arrow) and bottom: merger of both channels. Body axes (a: anterior; p: posterior; d; dorsal; v: ventral) are shown.

Results

We used this approach to photocontrol the activity of a Cre/loxP recombination system in a transgenic zebrafish line (Tg(*actin*:loxP-EOS-stop-loxP-KRASG12V-T2A-H2B-mTFP; *ubi*:Cre-ERT; *myl7*:EGFP) carrying a floxable (loxP flanked) EOS gene (coding for a green fluorescent protein) upstream from the oncogene[33,34] (KRASG12V). In such a transgenic zebrafish line hereafter referred as KRASG12V line (**Fig.1B**, **Fig.S1B**) the expression of EOS can be switched to KRASG12V and H2B-mTFP (nuclear blue fluorescence) upon light-mediated uncaging of cCYC and CRE-ERT activation (**Fig. 1C**); mTFP fluorescence can be observed about 30min post-illumination (**Fig. S1B**) and is stably maintained in zebrafish (**Fig. S1C**). Consistent with an acquired refractory cell state and a loss of oncogenic competence[30], whole body expression of the oncogene at 1dpf did not result in tumorigenesis.

To test for the possible impact of a reprogramming factor on the malignant transition, embryos from this transgenic line were injected at the one-cell stage with the mRNA of a construct consisting of a glucocorticoid receptor (GR) fused with a reprogramming factor (Ventx, Nanog or Oct4)[24,37] (**Fig. S3**). The resulting protein (e.g. Ventx-GR) is sequestered by cytoplasmic chaperones and transiently activated upon incubation of zebrafish in Dexamethasone (Dex) (**Fig. S2A**). Activation of the oncogene[33] at 1dpf, only if followed by transient activation of Ventx (or Nanog or Oct4) did yield reproductible hyperplasic outgrowths (**Fig. S3B-E**). Immuno-histo-chemistry detection of phospho-ERK activity (**Fig. S4A**), Hematoxylin & Eosin staining (**Fig. S4B**) and RT-qPCR of selected genes (**Fig. S5** and **S6A,B**) all display features associated with tumorigenesis. None of the controls (activation of kRasG12V only, Ventx-GR only, incubation in cyclofen or dexamethasone, etc.) developed hyperplasia, but rather grew into normal zebrafish (**Fig. S3**).

Since both kRasG12V and Ventx have been reported to play a role in brain cancer[38], we decided to activate the oncogene kRasG12V at 1dpf in a single normal cell of the brain of a transgenic zebrafish (injected with the mRNA of Ventx-GR at 1 cell stage). Activation of the oncogene in a single cell was achieved by illumination at 405nm to uncage cCyc in a small region (diameter ~80 μm) of the brain (in the vicinity of the otic vesicle) (**Fig. 1**). On average the oncogene is then activated in a single cell, identified within ~1h by the blue fluorescence of its nuclear marker (H2B-mTFP), see **Fig. 1**. Notice that single-cell activation of the oncogene alone does not give rise to cancer (**Fig. S8A**). However, if following the local expression of the oncogene (and its fluorescent marker), Ventx-GR is transiently activated the cell divides and proliferates (**Fig. 2**). We observed that at 1-day post induction (dpi) 50% of the induced cells had divided and expanded clonally by a factor ~3 (**Fig. 2B**), while the other 50% had neither divided nor died. Surprisingly, at 3-5 dpi, we observed in all zebrafish larvae that the induced cell gave rise to progeny that display short-range dispersion (**Fig. S7A, B**) and then give rise to a tumor mass in the brain with local infiltration of malignant cells (**Fig. 2C**). Hematoxylin-Eosin (H&E) staining of the brain tissue (**Fig. 2D, E**) and metastases (**Fig.3**) further confirm the malignant state of the induced cell and its progeny.

In parallel with tumor mass formation in the brain (**Fig. 2**), we observed that some cells of the progeny re-localized to new loci far from the brain, such as the heart (**Fig. 3A**), the digestive tract (**Fig. 3B**, **Fig. S6D**) and the trunk (**Fig. S6C**). We therefore deduce that the transient activation of Ventx alters the state of a cell expressing a mutated oncogene (i.e. KRASG12V) and induces its malignant transformation *in vivo*, with tumorigenic potential and the capacity to generate invasive progeny.

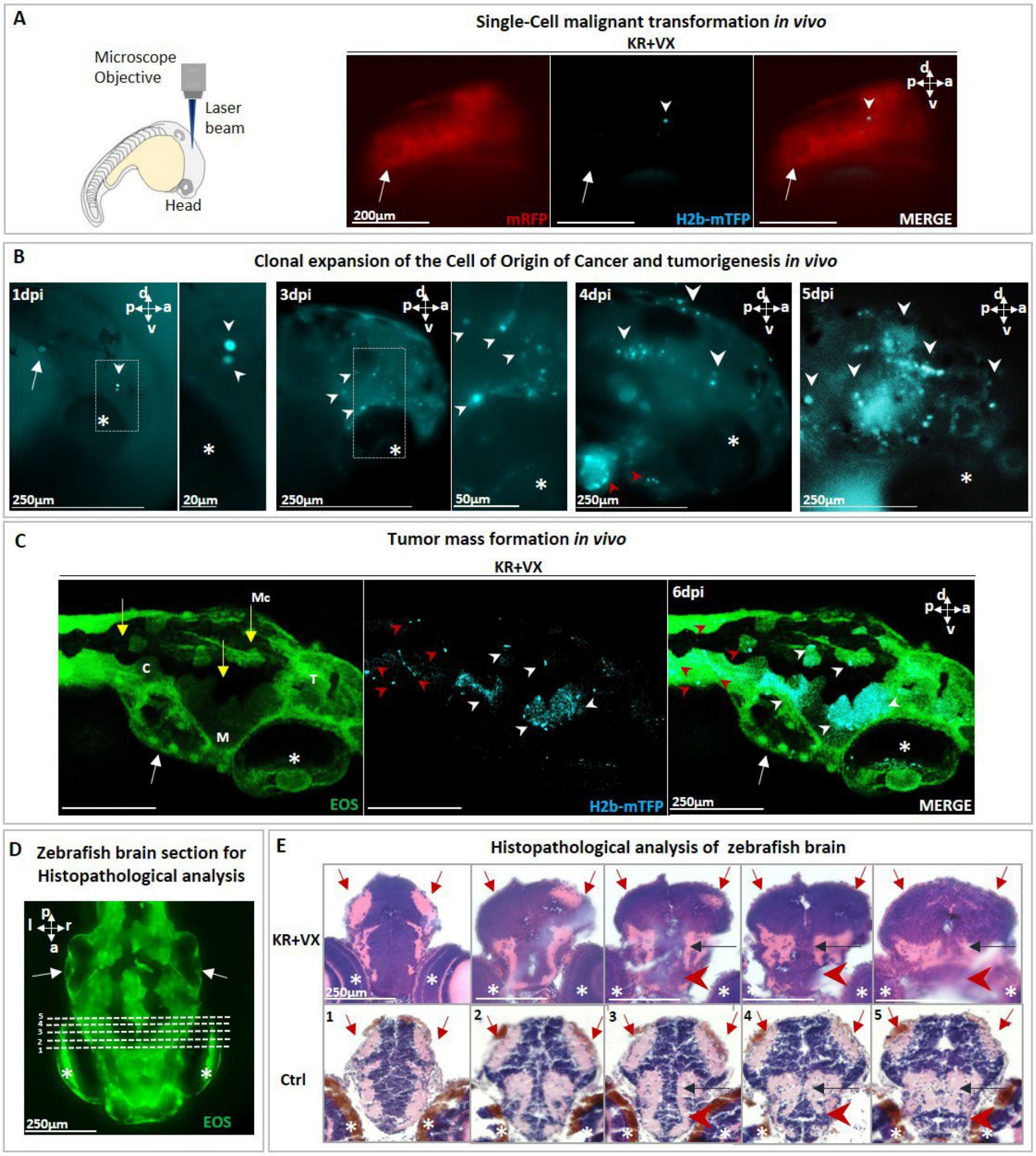

FIGURE 2

Malignant transformation of a single cell triggering carcinogenesis *in vivo*.

(A) At 1dpf, a single cell in a zebrafish brain was photo-induced to express the oncogene KRASG12V, identified (white arrowhead) within ~1h by the fluorescent H2B-mTFP. Membrane-bound mRFP is used as tracer. Transient (24h) DEX activation of Ventx is done following photoactivation. **(B)** At 1day post induction (1dpi), the activated cell has divided, giving rise to two cells (white arrowhead). After 3dpi the original cell expanded clonally (white arrowheads) by short-range dispersal within the brain. At 4dpi the brain has been colonized (left panel) by the progeny of the activated cell (white arrowheads) that display tumor growth as well as dispersal in the head or entering into the cardiovascular system (red arrowhead). At 5dpi, a tumor mass is formed. **(C)** Confocal microscopy of a larval head displaying tumors (arrowheads) and dispersal in the trunk (red arrowheads). **(D)** Histopathological sections of larval brain (dorsal view). Dashed lines (1 to 5) indicates sections showed in **(E)** Hematoxylin & Eosin (H&E) staining of brain at 5dpi of KR+VX-induced larva (depigmented) is compared to normal brain (Ctrl, melanocytes in brown). At 5dpi, the optic tectum (red arrows), the tegmentum (black arrow) and hypothalamus (red arrowhead) are infiltrated by a dysplasic tumor, progeny of the initial induced single cell. An asterisk (*) indicate the eye and a white arrow the otic vesicle. Scale bars and the body axes (a: anterior; p: posterior; d; dorsal; v: ventral) are shown. T=telencephalon; M=Mesencephalon; C= Cerebellum; Mc= Melanocytes.

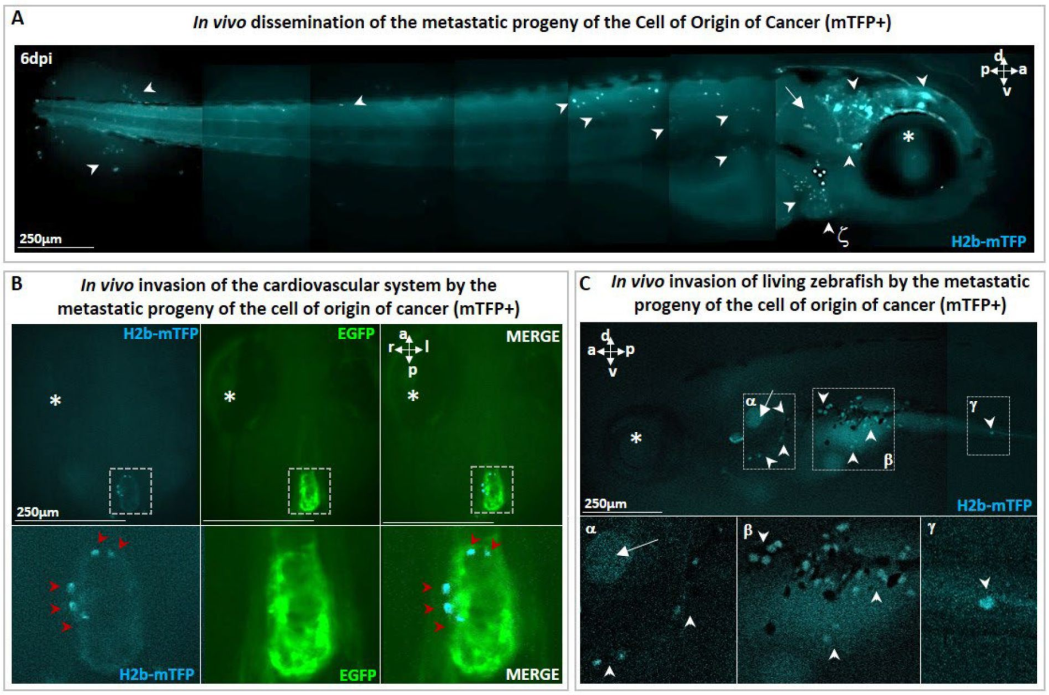

FIGURE 3

Metastatic cells following single cell malignant transformation.

(A) A zebrafish larva, in which a single cell in the brain was photo-induced (at 1dpf) to express the oncogene KRASG12V by the blue fluorescence of the expression marker (H2b-mTFP) as in (**Fig. 2**), show that the progeny of the Cell of Origin of Cancer give rise to a tumor mass in the brain (white arrowhead), as well as to migrating metastatic-like cells that disseminate in the whole organism (white arrowhead), some localizing in proximity of arterial branchial arches (indicated by ζ and white arrowhead), trunk and tail fin. **(B)** H2b-mTFP positive cells can migrate far from the site of induction (brain) and colonize ectopic tissues located in the heart and **(C)** the bottom of otic vesicle (in proximity of the primary head sinus, designated by α), the digestive tract (designated by β and γ) a feature characteristic of metastatic cancer cells. Note that no anaesthetics (e.g. tricaine) or mounting media (low melting point agarose or methylcellulose) were used to block live zebrafish, during both monitoring and imaging performed on live zebrafish. An asterisk (*) indicate the eye and a white arrow the otic vesicle. Scale bars and body axes (a: anterior; p: posterior; d; dorsal; v: ventral) are indicated.

Of the larvae in which a single cell was expressing the oncogene and in which Ventx was transiently activated (KR+VX cell), all (n=15) developed tumors within 5 dpi. The frequency of tumor development is therefore F_1=1. Conversely the probability for such a cell to not develop a tumor is F_0=0. Due to the finite size of the sample, we estimate the probability of tumor development from a single cell to be: P_1 > 80% (χ^2 = 3,75; df=1).

To definitely confirm the carcinogenic nature of the KR+VX induced cells we isolated and injected a single cell from a hyperplasic tissue (identified by the blue fluorescence of its nucleus) into a naïve host zebrafish larva. This led to integration, migration and colonization of the host tissues by the progeny of the transplanted cell (**Fig. 4A,B**), with strong pERK activity detected in tumor masses of the host (**Fig. 4B**). Out of 52 transplanted host zebrafish, 31 developed tumors, a probability of tumor development (60%) consistent with previously reported efficiency of tumor cells transplantation in zebrafish[39]. This result definitely confirms the cancerous nature of cells expressing a mutated oncogene and exposed to the transient activation of Ventx, with subsequent alteration of the homeostasis. Notice that injection into a naïve larva of an oncogene expressing cell (identified by its nuclear blue fluorescence) which did not experience the transient activation of a reprogramming factor does not yield a tumor (**Fig. S7B**).

Discussion

The surprising frequency of somatic mutations occurring in physiologically normal tissues[40,41] raises the question of what combinations of events are sufficient for the malignant transformation of a single cell and the rise of the cell of origin of cancer. The robust deterministic process of single-cell cancer induction that we uncovered suggests that the aberrant reactivation of Epi-Driver genes involved in reprogramming/pluripotency (such as VENTX/NANOG, POU5/OCT4) might be relevant to the irreversible malignant transformation of a cell. Reprogramming Epi-Drivers are important regulators of cell viability, survival and proliferation in several cellular contexts, from embryonic stem cells to cancer cells[22-27]. Due to their capacity to modulate epigenetic memory and cell plasticity, these reprogramming factors may drive the early stages of malignant transformation *in vivo* once (re)activated aberrantly. They likely share some mechanism(s) with processes such as induced nuclear-reprogramming[22,23,24], pluripotency maintenance and/or endogenous cell reprogramming during development[37]. Thus, consistent with our results, the reactivation[37] of the Neural Crest (NC) Progenitor program (possibly via the stochastic expression of VENTX/NANOG and/or POU5/OCT4) has been shown in BRAF/p53 double mutant cells to yield NC-related tumors *in vivo*[30-32].

Since cells carrying cancer-causing mutations do not deterministically developed cancers *in vivo*[32,40], *we suggest that the probability of a mutated cell to enter into malignant transformation, or to maintain its physiological functions despite mutations, correlates with the probability of the reactivation of reprogramming factors. Our results support a "Vogelgram"[42] two-step model (**FIG. 5**) for irreversible single-cell malignant transformation in vivo*, mirroring the two hits hypothesis proposed by Berenblum and Shubik[43].

Thus, the appearance of Mut-Drivers in a normal (preprocancer[41]) cell[40] within healthy tissue would act as a permissive but insufficient initiator for malignant cell transformation. Despite the frequency of mutational insults, which are often caused by external cues (chemical carcinogens, UV, etc…) or senescence/ageing, it is known that surveillance mechanisms like cell competition between wild-type and mutated cells safeguard tissue homeostasis and results in active elimination of mutant cells from the tissue[44,45,46]. Our data imply that the aberrant reactivation of Epi-Driver genes involved in reprogramming/pluripotency may promote the irreversible and deterministic malignant transformation in the cell of origin of cancer leading to carcinogenesis.

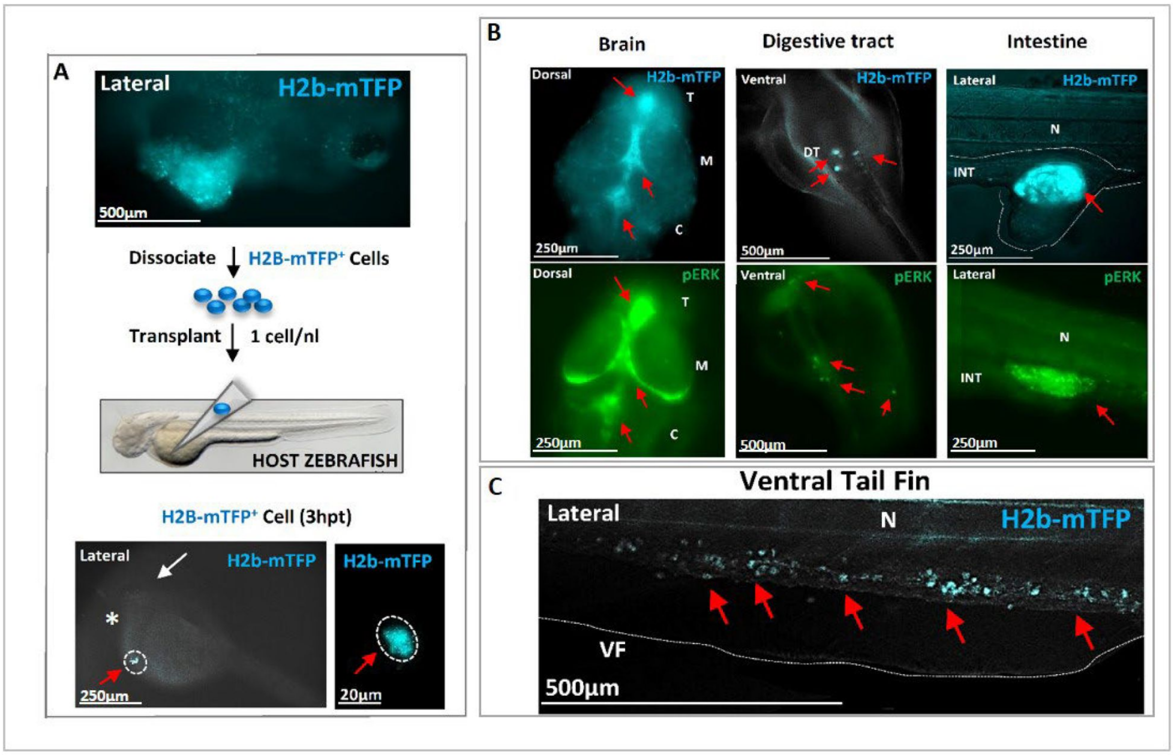

FIGURE 4

Transplantation of single cell(s) from hyperplasic tissue reveals cancer-initiating potential.

(A) Following KRASG12V *plus* Ventx activation, hyperplasic tissues (blue fluorescent) are observed at 6dpf, top figure. The cells of the hyperplasia were dissociated and isolated blue (KRAS expressing) cells were transplanted (≈ 1 cell *per* host) at 2dpf in a *Nacre* (*mitf* -/-) zebrafish line for a better tracking of the transplanted cells. The transplanted H2b-mTFP positive (blue) cell (red arrow) can be visualized as early as 3 hours post transplantation (3hpt) in the yolk of the host, close to the duct of Cuvier. White arrow indicates the head/eye (lateral view). **(B)** At 3 dpt the blue cell(s) from the hyperplasic tissue of the donor have colonized the host *Nacre* zebrafish larvae. Tumors in the brain, digestive tract and intestine, are observed and characterized by the blue fluorescence of the donor KRAS expressing cells (red arrows; n=31 out of 52 host individuals). In the bottom, immunofluorescence (IF) analysis of representative host zebrafish larvae with specific high level of phosphorylated ERK activity (pERK, red arrows) in the brain, intestine and digestive tract. **(C)** A high number of exogenous blue fluorescent cells are here observed to migrate in the tail (red arrows). These observations indicate that the transplanted founder cell has both migratory, colonizing behavior, as well as survival growth advantage in the host to form tumors, and thus to re-initiate carcinogenesis. Scale bars and body axes (a: anterior; p: posterior; d; dorsal; v: ventral) are shown; T=telencephalon; M=Mesencephalon; C= Cerebellum; N=notochord; VF= ventral fin.

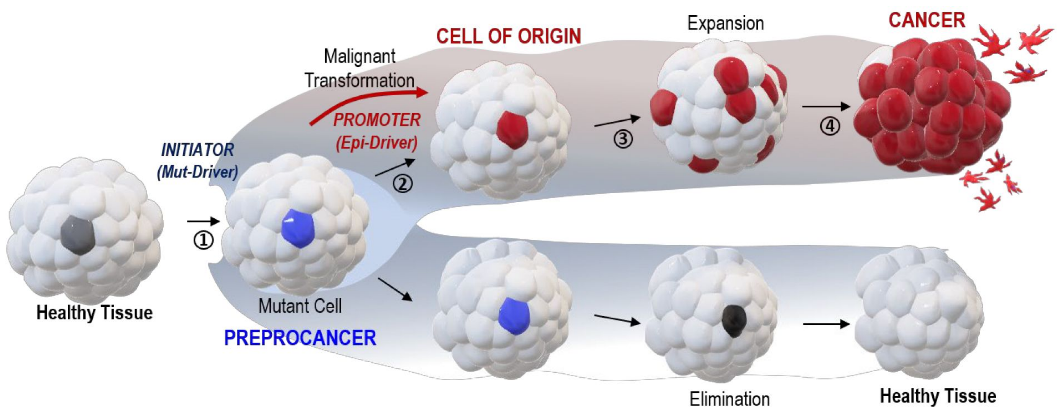

FIGURE 5

A two-steps "Vogelgram" model of deterministic and irreversible single-cell malignant transformation *in vivo*.

Within a healthy tissue, a normal cell (in light grey) acquires (step 1) genetic mutation(s) in driver oncogene(s) (Mut-Drivers such as kRASG12V). Such a mutant cell (in blue, referred as a preprocancer[41] cell) can (step 2) aberrantly activate the expression of Epi-Drivers involved in pluripotency/reprogramming (e.g. VENTX/NANOG, POU5/OCT4) thus undergoing deterministic and irreversible malignant cell transformation (red cell, the Cell of Origin of Cancer); (step 3) *in situ* short-range dispersal of the early malignant cells and (step 4) further progression to cancer mass and to the appearance of metastatic cells. Inversely, the mutant (preprocancer) cell (in blue) can maintain its physiological functions and be eventually eliminated from the healthy tissue.

Our hypothesis is further strengthened by the observation that the variation in cancer risk among tissues can be related to the number of stem cell divisions and tissue renewal[6]. The aberrant reactivation (or maintenance) of Epi-Driver genes in these regenerative events, in cooperation with incident mutations, might be the key deterministic factor in the switching of a normal/healthy cell into the first cell of origin of cancer.

Furthermore, the results reported here are compatible with the recently proposed "ground state theory of cancer initiation7". According to that theory a malignant transformation may occur in a cell harboring an oncogenic mutation upon a change of its functional state (its "ground state"). Here the transient activation of a reprogramming factor (i.e. Ventx, Nanog or Oct4) possibly synergizes with the oncogene to alter the epigenetic and functional state of the cell allowing its transformation into a tumorigenic cell.

Importantly, our observation that the progeny of the cell(s) of origin of cancer display a short-range dispersal within the tissue during the earliest phases of tumorigenesis and prior to the effective appearance of tumor mass corroborates a recent theoretical model predicting such an early dispersal during carcinogenesis to explain heterogeneity, therapeutic resistance and tumor relapse[8].

Being the first experiments to predictably control the malignant transformation of a single cell in an unaltered microenvironment our approach opens a new vista on the study of "the cell of origin of cancer"[47], an acknowledged enigma of cancer research. As such our results raise many questions: what mechanisms are at work in the transition from the preprocancer state to a tumorigenic state? Is the aberrant reactivation of reprogramming factors a key step in the initiation of carcinogenesis, independent of age, tissue or oncogenic mutation? Do drugs against reprogramming factors reduce the probability of carcinogenesis? Conversely, do some carcinogens (e.g. environmental pollutants, pesticides, endocrine disruptors etc…) act by reactivating those factors?

By allowing for specific and reproductible single cell malignant transformation *in vivo*, our optogenetic approach opens the way for a quantitative study of the initial stages of cancer at the single cell level (e.g. tracking and characterization), that will allow one to address many of these questions.

Materials and methods

Fish lines and maintenance

Zebrafish were raised and maintained in an approved Fish Facility (C75-05-32 at IBENS) on a 14–10 h light-dark diurnal cycle with standard culture methods[48]. Embryos collected from natural crosses were staged according to Kimmel[49]. The Tg(*actin*:loxP-EOS-stop-loxP-KRASG12V-T2A-H2B-mTFP) was generated by injecting the plasmid pT24-*actin*:loxP-EOS-stop-loxP-KRASG12V-T2A-H2B-mTFP, which contains the homologous cDNA sequence of KRASG12V from human, with tol2 mRNA transposase. Founder transgenic fish were identified by global expression of Eos. The Tg(*ubi*:Cre-ERT; *myl7*:EGFP) was previously described[50]. The double transgenic line Tg(*actin*:loxP-EOS-stop-loxP-KRASG12V-T2A-H2B-mTFP; *ubi*:Cre-ERT; *myl7*:EGFP) was created by crossing Tg(*actin*:loxP-EOS-stop-loxP-KRASG12V-T2A-H2B-mTFP) and Tg(*ubi*:Cre-ERT; *myl7*:EGFP). Founder double transgenic fish were selected by global expression of Eos and expression of EGFP in the developing heart. Zebrafish were imaged for phenotypic analysis throughout early development, from embryonic to larval stage, and then fixed (at 6dpf) with PAXgene Tissue Container Product (Qiagen) for RT-qPCR or with 4% PFA (Thermofisher) for histological (Hematoxylin & Eosine, H&E) analyses.

Dexamethasone induction

transgenic zebrafish were injected at the one cell stage with the mRNA of a gene-construct Ventx-GR (*Xenopus* ventx2, 450pg), Nanog-GR (mouse Nanog, 100pg) or Pou5/Oct4 (*Xenopus* pou5f3.1/oct91, 100pg) together with a red fluorescent expression marker mRFP (50 pg). The protein products of these constructs are sequestered by cytoplasmic chaperones and released upon incubation of the embryos in a medium containing 10 μM Dexamethasone (DEX). In single cell activation experiments, zebrafish were selected from their strong intensity of fluorescent mRFP signal for local activation of kRasG12V via uncaging of 6μM cCYC (a gift of I.Aujard and L.Jullien).

Reverse transcriptase quantitative PCR (RT-qPCR)

Zebrafish larvae were fixed (as mentioned above) at 6 dpf. Total RNAs were extracted using the RNeasy micro kit (Qiagen) according to the manufacturer's protocols. Sample quantity and purity, reverse transcription, pre-amplification and High throughput qPCR were performed as in Zhang et al.[51]. Quantitative PCR was performed using the high throughput platform BioMark™ HD System and the 48.48 GE Dynamic Arrays (Fluidigm). RTqPCR measurements were done in triplicate on pooled zebrafish larvae and single zebrafish larva (for KR+VX condition), as indicated in the text. Normalization and quantification were obtained with the Δ(ΔCt) method using *rpl13a* as a reference gene.

Immunohistochemistry (IHC)

The zebrafish obtained in the various conditions and the stages mentioned in the text were fixed in 4% PFA overnight at 4 °C, followed by dehydration with 100% methanol at −20 °C for more than 1 day. After gradual rehydration of methanol and wash with PBS/Tween 0.1%, the embryos were incubated in a blocking solution: 1%Triton, 1% DMSO, 1% BSA and 10% sheep serum (Sigma) in PBS on a shaker for 1 h at room temperature, followed by incubation on a shaker overnight at +4°C with 1:500 anti-phospho-Erk antibody (phospho-p44/42 MAPK (Erk1/2) (Thr202/Tyr204) (D13.14.4E) XP®). Rabbit mAb detects endogenous levels of p44 and p42 MAP Kinase (Erk1 and Erk2) when dually phosphorylated at Thr202 and Tyr204 of Erk1 (Thr185 and Tyr187 of Erk2), and singly phosphorylated at Thr202 - this antibody does not cross-react with the corresponding phosphorylated residues of either JNK/SAPK or p38 MAP kinases) (ref 4370S Cell Signalling). After washing with PBS/Tween, embryos were incubated overnight at +4°C with 1/1000 secondary fluorescent conjugated antibody, Donkey anti-Rabbit Alexa Fluor 488 (Thermo Fisher A-21206). To visualize the distribution of Ventx-GR in the fish, embryos were incubated with 1:500 anti-HA antibody, tagging the HA sequence fused to Ventx-GR, as the conjugated antibody (Anti-HA, mouse IgG1, clone 16B12 Alex Fluor™ 488 conjugated, Thermofisher Ref. A21287) on a shaker overnight at 4 °C. All images were taken on a Nikon Ti microscope equipped with a Hamamatsu Orca camera, except for confocal microscopy (**Fig.2C**, S4B) carried out on a Leica SP5 and Zeiss LSM800 microscope.

Caged Cyclofen (cCYC) treatment and UV uncaging

To induce kRASG12V expression, 24hpf embryos were directly incubated in 6μM caged cyclofen (cCYC) for 1 hour (in the dark), briefly rinsed in E3 medium followed by 5 min. photo-activation with a ~365 nm UV lamp. They were then transferred back to E3 medium + 10 μM DEX (to release Ventx-GR from its complex with cytoplasmic chaperones). The embryos at 1 dpi were washed 3x in E3 medium to remove DEX. For this experiment, we used a benchtop UV lamp (Fisher VL-6-L) which emits a peak wavelength at 365 nm with a FWHM (full width at half maximum) of 40 nm and delivers on the illuminated sample a typical photon flux of ~4.3 Einstein/(s·m[2]).

Localized uncaging was performed by illumination for 7 min on a Nikon Ti microscope equipped with a light source peaking at 405 nm, **Fig.1**. The size of the uncaging region was controlled by an iris that defines a circular illumination of diameter ~ 80 μm. After 0,5-1 h following uncaging the illuminated region of each embryo was imaged to identify and count mTFP positive cell(s). Embryos were transferred to a 12-well plate with E3 + 10 μM DEX, incubated in total darkness overnight and washed 3x with E3 at 1 dpi (to remove DEX).

Cell transplantation

Zebrafish larvae were grown until 6dpi, dissociated in dissociation medium[52] (025% trypsin-EDTA *plus* 1/10 Collagenase 100mg/ml) 10min at 30°C, mechanically homogenized, resuspended in DMEM-10% Fetal Bovine Serum (FBS), filtered through 70μm nylon mesh (Corning Cell Strainer Ref. 431751) and resuspended in DMEM-10% FBS at 1cell/1nl concentration by using LUNA- II cell counter (Logos BioSystem).

Microscopy

Fluorescent images were taken on a Nikon Ti microscope equipped with a Hamamatsu ORCA V2+ camera and a 10X plan fluo objective. Filter setting of CFP: excitation at 438 ± 24 nm, emission at 483 ± 32 nm; mEosFP and Alexa 488: excitation at 497 ± 16 nm, emission at 535 ± 22 nm. Image analysis was done using ImageJ software.

Acknowledgements

We acknowledge financial support from the ITMO Cancer of Aviesan within the framework of the 2021-2030 Cancer Control Strategy, on funds administered by Inserm. The gene expression analysis was carried out on the high throughput qPCR-HD-Genomic Paris Centre core facility and was supported by grants from the Région Ile de France. We are grateful to I.Aujard and L.Jullien (ENS, Dept. of Chemistry) for a gift of caged cyclofen. We acknowledge useful comments on a draft of this paper by Z.Feng, M.Distel and D.Louvard. P.S. acknowledges useful discussions with C. Rogard, M. Smilla, L.A.M. Scerbo and E.P.A. Scerbo. We thank the Graphic Atelier of Timon Ducos for scientific illustrations (*https://timonducos.com/*).

Supplementary figures

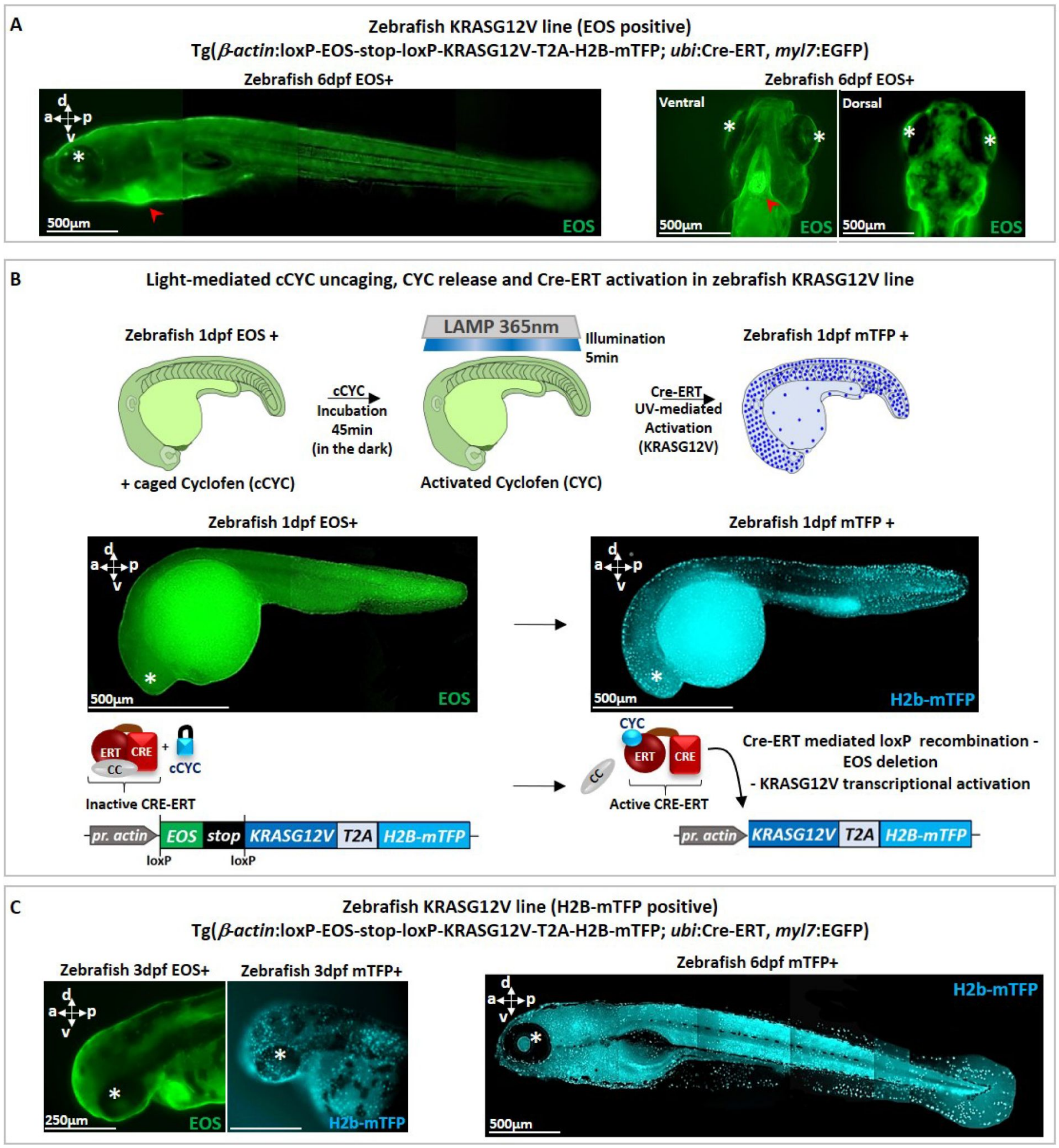

FIGURE S1

Characterization of the double transgenic line Tg(β−*actin*:loxP-EOS-stop-loxP-KRASG12V-T2A-H2B-mTFP; *ubi*:Cre-ERT; *myl7*:EGFP).

(A) A transgenic fish at 6dpf displays green EOS fluorescence throughout the body and a strong green fluorescence in the heart due to the additive expression of EGFP under a heart specific (*myl7*) promotor, red arrowhead. **(B)** Upon global illumination (at 1dpf) with a ~365nm UV lamp in presence of cCYC, cyclofen is uncaged which releases CRE-ERT from its complex with cytoplasmic chaperones and results in floxing of EOS and ubiquitous expression of KRASG12V and H2B-mTFP. The embryos thus display blue fluorescence in the nuclei shown here at 1h post induction (hpi). (**C**) Stable and ubiquitous expression of the blue H2B-mTFP fluorescent protein in zebrafish late embryos (3dpf) and larvae (6dpf). Note that in all pictures the asterisk (*) indicate the eye. Scale bars and body axes (a: anterior; p: posterior; d; dorsal; v: ventral) are shown.

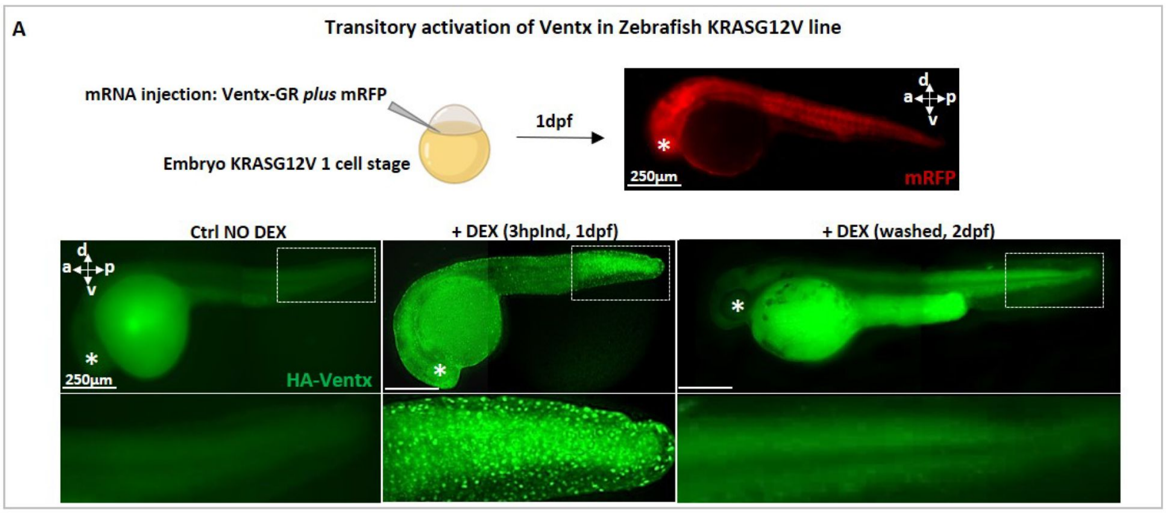

FIGURE S2

Transient activation of Ventx reprogramming factor.

(A) top: At one cell stage Ventx-GR mRNA is injected together with mRFP mRNA (used as a tracer), which expression throughout the embryo (here shown at 1dpf) is a proxy for Ventx-GR expression. **Bottom:** Immunofluorescence analysis show that Ventx protein can be visualized in fixed embryos with the help of an antibody (Ab) directed against the HA tag linking Ventx and GR (and visualized by a second Ab linked to a green fluorescent marker). Upon addition of DEX at 1dpf embryos, Ventx is released from its complex with cytoplasmic chaperones and diffuses into the cell nucleus, resulting in a pointillist image of the nuclei (middle). At 2dpf, after washing out DEX, Ventx protein is no longer detected and the pointillist image is lost (right). Note that in all pictures the asterisk (*) indicate the eye. Scale bars and body axes (a: anterior; p: posterior; d; dorsal; v: ventral; l: left; r: right) are shown.

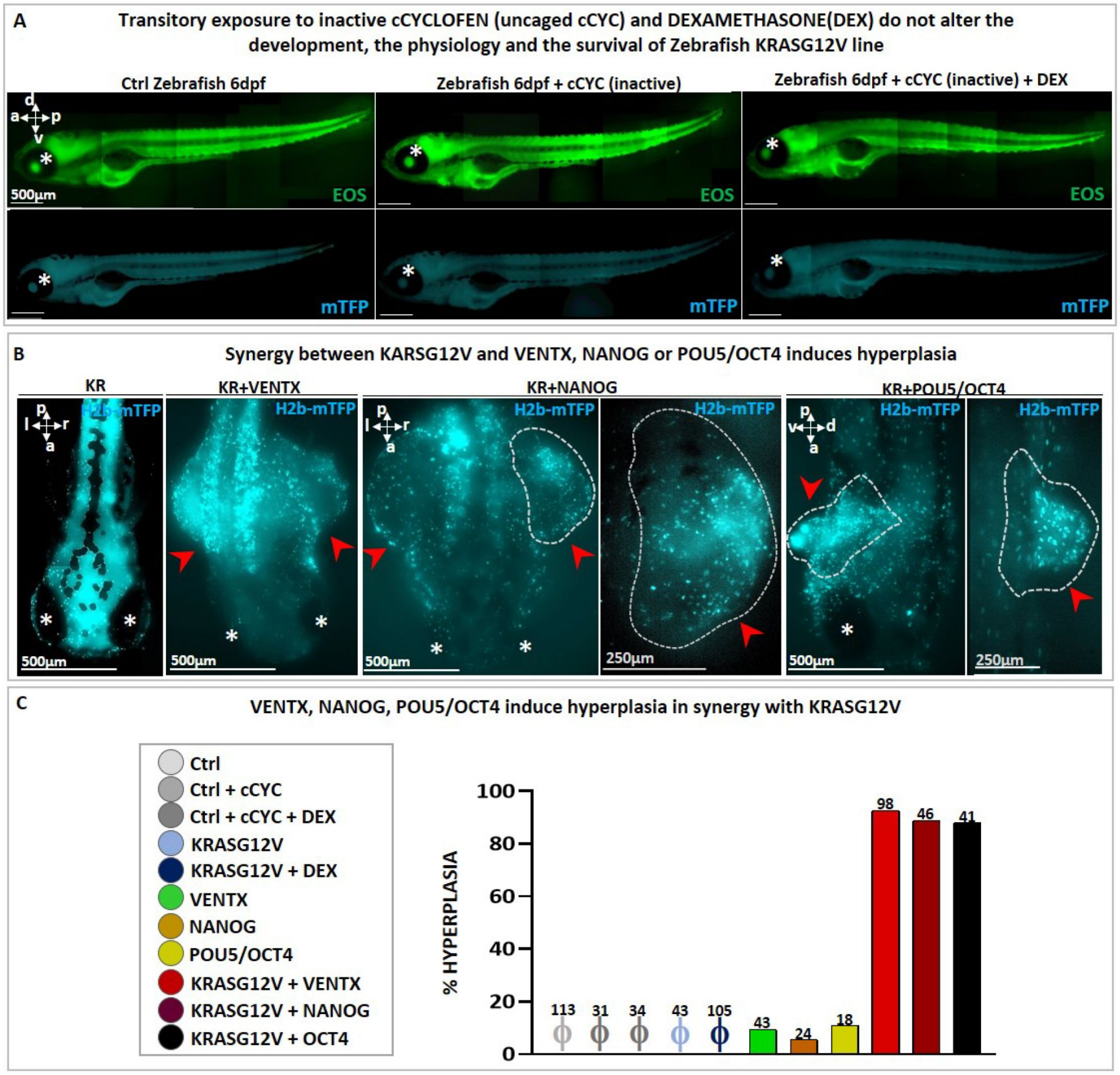

FIGURE S3

Synergy between a reprogramming factor and KRASG12V oncogene efficiently induces tumors in zebrafish larvae.

(A) Images of control zebrafish larvae at 6dpf: without any treatment (left), with transient incubation in cCYC (without UV, middle) and with incubation in DEX + cCYC (without UV, right). Note that zebrafish does show neither morphological anomalies nor mortality. **(B)** Photoactivation (*via* cCYC uncaging and Cre-ERT activation) of KRASG12V (blue nuclei) in 1dpf zebrafish without (left) or with subsequent transient activation (right) of Ventx-GR by Dexamethasone (DEX) (described in **Fig. S2**). These larvae (labelled as KR+VX) develop hyperplasic tissues within 6-9 dpf (dorsal view, red arrows indicate hyperplasia). Photoactivation (*via* cCYC uncaging and Cre-ERT activation) of KRASG12V (blue nuclei) in 1dpf zebrafish with subsequent transient activation of NANOG-GR or POU5/OCT4-GR by Dexamethasone (DEX) (set-up described in A). These larvae (labelled as KR+NANOG or KR+POU5/OCT4) develop hyperplasic tissues within 6-9 dpf (dorsal view, red arrows indicate hyperplasia). **(C)** Quantification of zebrafish developing abnormal hyperplasia upon the indicated treatments. Note that only the synergy between reprogramming factors (i.e. VENTX, NANOG or POU5/OCT4) and the KRASG12V oncogene reproducibly and efficiently induce tumors in zebrafish larvae. The total number of zebrafish larvae analyzed are indicated above the bars. φ indicates no event (0%). Note that in all pictures the asterisk (*) indicate the eye. Scale bars and body axes (a: anterior; p: posterior; d; dorsal; v: ventral; l: left; r: right) are shown.

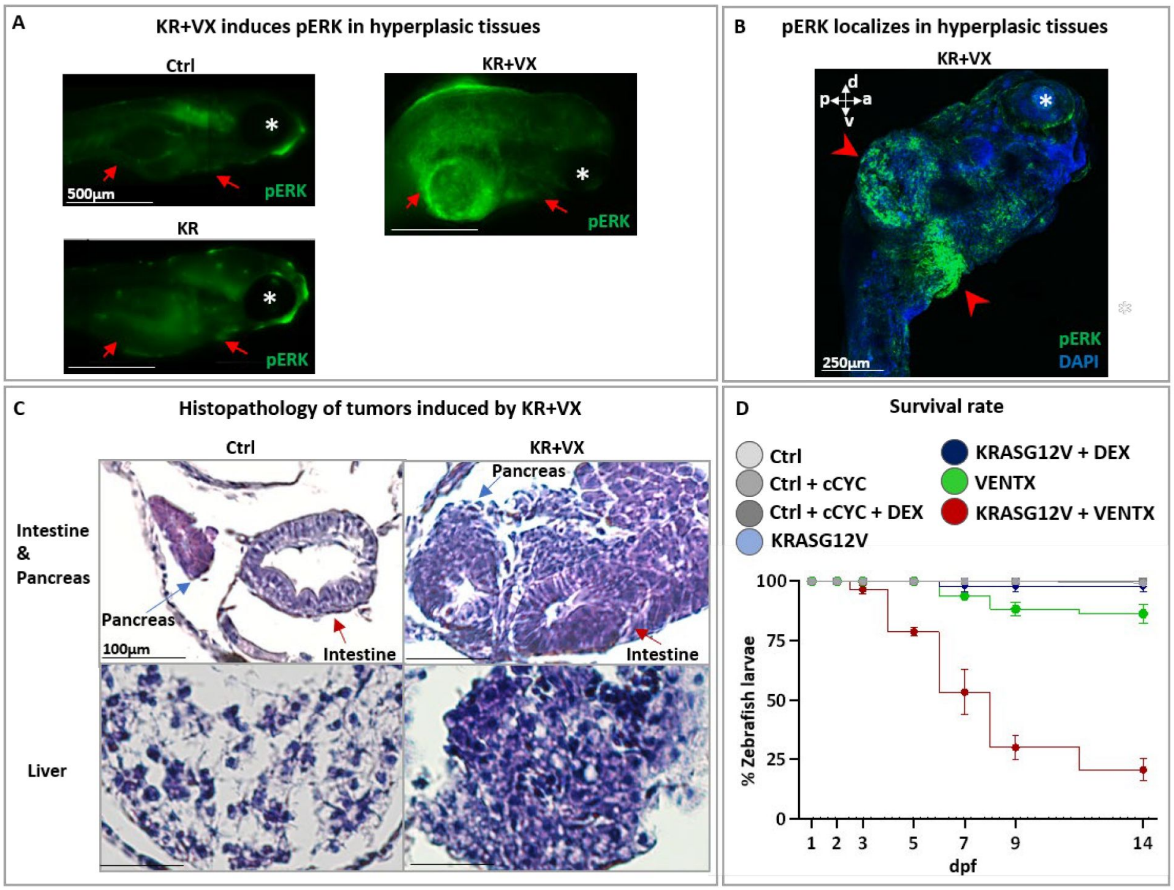

FIGURE S4

Synergy between the Ventx reprogramming factor and the KRASG12V oncogene induces tumors in zebrafish larvae.

(A) Phosphorylated ERK (pERK) immunofluorescence at 6dpf in non-activated larvae (Ctrl), in larvea in which only KRASG12V was activated (KR) and in larvae in which both KRASG12V and VENTX were activated (KR+VX). Notice in the last one the strong pERK activation in the hyperplasic abdominal outgrowth. The digestive tract is shown between the red arrows. **(B)** Confocal microscopy of KR+VX zebrafish larva at 6dpf (ventro-lateral view) displays the immunofluorescence of active phosphorylated ERK (pERK, in green and indicated by red arrowheads) in the abdomen of a DAPI labelled zebrafish larva. **(C)** Histopathological analysis by Hematoxylin & Eosin (H&E) staining of hyperplasic tissues in zebrafish larvae (6dpf) upon activation of KRASG12V *and* Ventx (KR+VX) is compared with normal tissues (Ctrl). Larvae overexpressing KR+VX develop hyperplasic and dysplastic cancer-like features and tissue outgrowth in the gut/intestine (red arrow), pancreas (blue arrow) and liver. **(D)** Such cancer-like features specifically and exclusively reduce the survival rate to 20% two weeks after induction.

	Controls			kRas activated		Ventx activated	kRas and Ventx activated	
		+cCyc	+cCyc+Dex	+cCyc+UV	+cCyc+UV+Dex	+Ventx +Dex	+cCyc+UV+Ventx+Dex	
	Δ<ΔCt>	Δ<ΔCt>	Δ<ΔCt>	Δ<ΔCt>	Δ<ΔCt>	Δ<ΔCt>	Δ<ΔCt>	
foxo3a	0,04872021	0,066813631	-0,03884898	-0,293118511	-0,271524182	-0,155890847	-1,451581111	foxo3a
Fgf8a	-0,0316562	-0,037978163	0,111695187	-0,139967188	0,096481912	-0,304560279	-1,276111195	Fgf8a
ved	-0,062319	0,056851534	0,038679369	-0,605958068	-0,513674812	-0,398838855	-1,036695128	ved
Igf1	0,07678058	0,032354068	0,083099625	0,12686197	0,024535274	0,07746345	-0,97453591	Igf1
lats1	0,03673484	-0,036669673	0,038736507	-0,098140475	-0,092443913	-0,23317429	-0,887730484	lats1
vent	-0,3169197	-0,000355943	-0,099617548	-0,579512277	-0,602491017	0,015225459	-0,867309319	vent
tet3	-0,0532106	0,079700505	0,078403895	-0,199526619	-0,131830261	-0,219438634	-0,863216001	tet3
dnmt3ab	-0,0357257	-0,006148767	0,118517492	-0,306617507	-0,141657287	-0,20957213	-0,732486941	dnmt3ab
dnmt3aa	-0,0504544	-0,007912781	0,199249632	-0,180455826	-0,217342227	-0,294476837	-0,628814611	dnmt3aa
ogt.1	0,00403322	-0,016473298	0,430023969	0,18988821	0,135000623	0,090384872	-0,60759739	ogt.1
Axin2	0,08603419	0,219359555	-0,013353283	-0,050856185	-0,104414079	-0,138752259	-0,538733241	Axin2
spop	-0,0300237	-0,019726405	0,120376946	-0,082633365	0,027495013	0,078957725	-0,491445824	spop
kdm4b/jmjd2b	-0,145206	0,080064866	0,097965065	0,061411636	-0,108485807	0,139577054	-0,412005559	kdm4b/jmjd2b
Rarab	0,02099564	0,051849194	0,038788116	-0,00784701	0,12754287	0,142057791	-0,326049965	Rarab
cdkn2c	0,00083528	-0,104997575	0,180454946	-0,005853341	-0,138413953	-0,200731873	-0,297559128	cdkn2c
vox	-0,1175871	0,133984924	0,048048575	-1,045092865	-0,251504612	-0,685830593	-0,25921086	vox
Ifg1rb	-0,0289123	0,048834808	0,16078023	-0,096388572	-0,341849175	0,280854532	-0,246962892	Ifg1rb
gadd45ab	0,21193642	-0,142790555	0,000837928	0,110408322	-0,003362872	0,012923136	-0,144044862	gadd45ab
kdm2aa	0,03744458	-0,006748344	0,172851727	-0,027779006	-0,022077261	0,086760839	-0,11435749	kdm2aa
Igf1ra	0,05350456	-0,046745285	0,186847232	0,043639861	0,015615143	0,306578599	-0,036438319	Igf1ra
Fgfr4	0,08649694	0,056311465	0,003024985	0,047292782	-0,101782633	0,024137795	-0,029594499	Fgfr4
mycb	0,18346869	-0,116571215	-0,091937315	0,072283059	-0,081705099	0,042206402	-0,024043298	mycb
Rpl13a1	0	0	0	0	0	0	0	Rpl13a1
Crabp2a	0,27396987	0,050644571	0,013698332	0,343274538	0,807447636	-0,193584098	0,076031348	Crabp2a
Rpl13a2	0,01121027	0,010510704	-0,001256252	-0,035641192	0,061076774	0,161298263	0,09356535	Rpl13a2
neil1	0,14237711	0,306303898	-0,136999316	-0,058829182	0,275602068	0,02413347	0,099200473	neil1
xpc	0,19850395	0,248807568	0,149025113	-0,326880665	0,245047865	-0,117565209	0,14401152	xpc
yap1	0,12663667	-0,403201384	0,029655143	0,063826641	-0,025913909	0,225475717	0,322245402	yap1
dnmt3ba	0,22320522	0,071212162	-0,022988627	-0,007797843	0,177840877	-0,038930578	0,362606864	dnmt3ba
tdg.1	-0,0146472	0,017439316	0,175740921	0,196956543	0,201735666	0,081400348	0,374643654	tdg.1
Dusp6	-0,0063794	0,008972899	0,145712401	0,180805923	-0,013383475	0,459206026	0,397476351	Dusp6
hdac1	0,01603162	0,050545015	0,126583039	0,274386372	0,363330409	0,120167688	0,459214036	hdac1
mycla	0,11142714	0,109093676	0,005002688	-0,016513835	0,346710069	-0,067904277	0,480061082	mycla
Fgf4	0,01546979	0,088487682	0,10653939	1,035851502	0,505450108	0,06236434	0,561289918	Fgf4
jmjd6	0,3797529	0,169448309	0,231656162	0,561245122	0,537658532	0,131190392	0,834967741	jmjd6
dnmt1	0,03127183	0,049585132	-0,001661771	-0,001552923	0,146168151	0,029219662	0,857301504	dnmt1
ezh2	0,03115227	0,119119745	0,304658216	0,42844819	0,807839789	0,123506921	0,956713342	ezh2
tert	-0,0967514	-0,003804735	0,045885003	0,084632262	0,426625459	-0,471192203	1,045527604	tert
Cyp26a1	0,31505339	-0,039886021	-0,190142549	-0,167616874	0,206061671	-0,213339056	1,084768891	Cyp26a1
gadd45aa	0,07051602	-0,057068036	0,256474599	0,700862593	0,670467445	0,779890562	1,15113207	gadd45aa
Crabp1b	0,1611499	0,151987902	0,008476803	0,476468009	0,606191919	0,202152011	1,163910911	Crabp1b
Aldh1a2	0,15447759	-0,016105716	0,069151831	0,070425488	0,338003042	-0,072082682	1,317325359	Aldh1a2
sall4	0,23727667	0,113398919	-0,156062592	0,237442763	-0,088303132	0,357457252	1,403750432	sall4
actb1	-0,0833952	0,037316906	0,115046858	0,662392235	0,686517859	0,013990979	1,553516271	actb1
dnmt3bb.1	0,33153617	-0,127283348	0,187090733	0,452419479	0,554407057	0,381311822	1,577691804	dnmt3bb.1
lin28a	0,06042223	0,118127006	0,127195634	0,003700138	0,35682603	-0,610713861	1,952949272	lin28a
pou5f3	-0,0230147	-0,158341164	-0,305969178	1,139832583	-0,395495353	1,118406228	2,635065729	pou5f3
nanog	0,20241131	0,293432699	0,14949247	0,832437293	0,931894166	1,367847209	3,179750609	nanog
				reprogramming genes	stemness gene	oncosuppressor	epigenetic memory	

FIGURE S5

KRASG12V *plus* Ventx induces a cancer-like gene expression signature.

Both KRASG12V *and* Ventx-GR (KR+VX) were activated in zebrafish at 1dpf. The larvae (n=24) were collected at 6 dpf and processed for RT-qPCR analysis. Compared to the controls (Ctrl ; Ctrl+ cCyc ; Ctrl + cCYC + Dex) and larvae in which only KRASG12V (+cCyc+UV; +cCyc+UV+ Dex) or Ventx (Ventx+Dex) were activated, the co-activation of KRASG12V + Ventx (+cCyc+UV+VentX+Dex) displayed significant changes in gene expression, with over-expression of genes involved in pluripotency/reprogramming (nanog, pou5f3/oct4, lin28) and stemness (aldh1a, tert) and under-expression of oncosuppressor genes (foxo3, lats1,spop) and genes involved in epigenetic memory (tet3, dnmt).

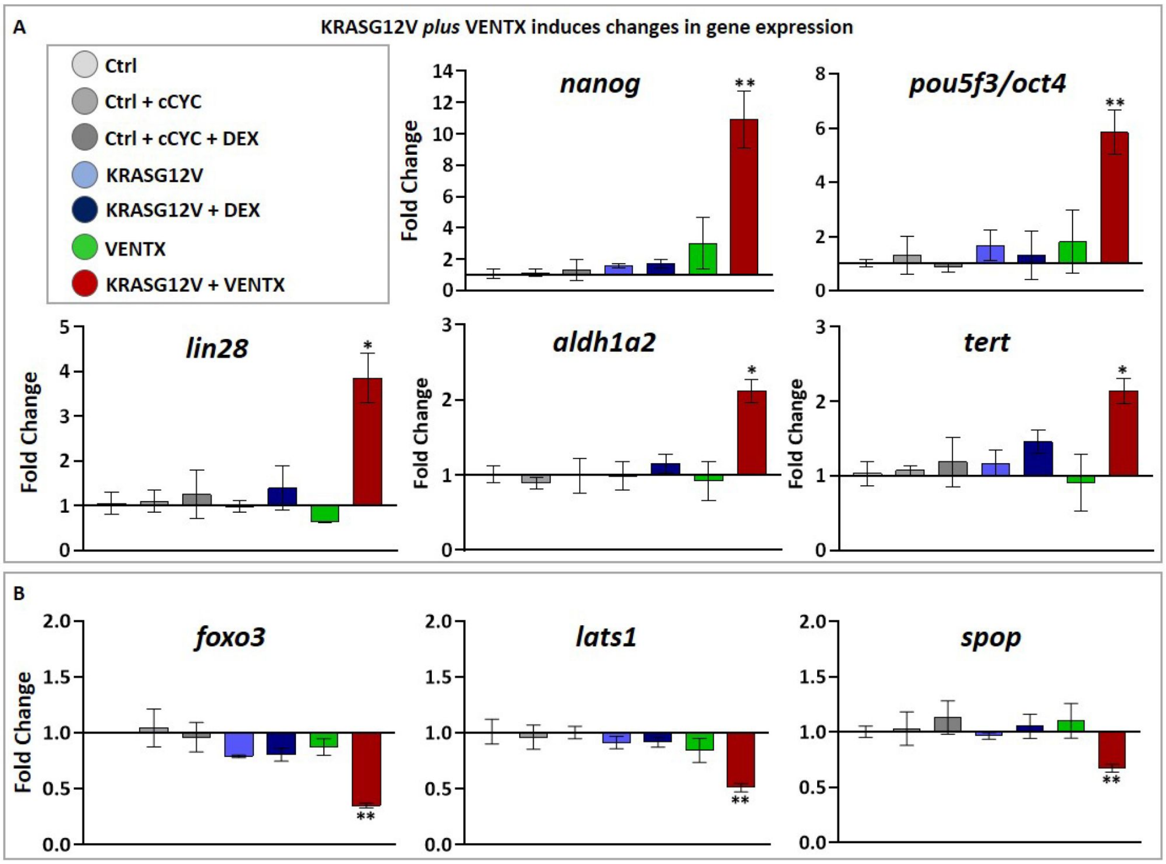

FIGURE S6

KRASG12V *plus* Ventx induces a cancer-like gene expression signature.

Some of the data shown in **Fig.S5** are here displayed with their error bars. Compared to the controls (Ctrl in light grey; Ctrl+ cCyc in grey; Ctrl + cCYC + DEX in dark grey) and larvae in which only KRASG12V (KRASG12V in light blue; KRASG12V + DEX in blue) or Ventx (VENTX in green) were activated, the co-activation of KRASG12V + VENTX (in red) displayed significant changes in gene expression. **(A)** Pluripotency/reprogramming factors like *nanog, pou5f3*/*oct4* and *lin28*, as well as stemness markers like *aldh1a2* and *telomerase* (*tert*) are significantly up-regulated ($p<0.05$, compared to Ctrl) by KR+VX but not by KRASG12V (KR) or Ventx (VX) alone. **(B)** Conversely, onco-suppressors such as *foxo3, lats1* and *spop* are significantly down-regulated ($p<0.05$) by KR+VX but not by KRASG12V (KR) or Ventx (VX) alone when compared to control. For all qPCR graphs, error bars represent s.e.m. values. For statistical analyses, samples were compared with the respective control by Unpaired Student's t-test. * $p<0.05$, ** $p<0.005$. *** $p<0.0001$.

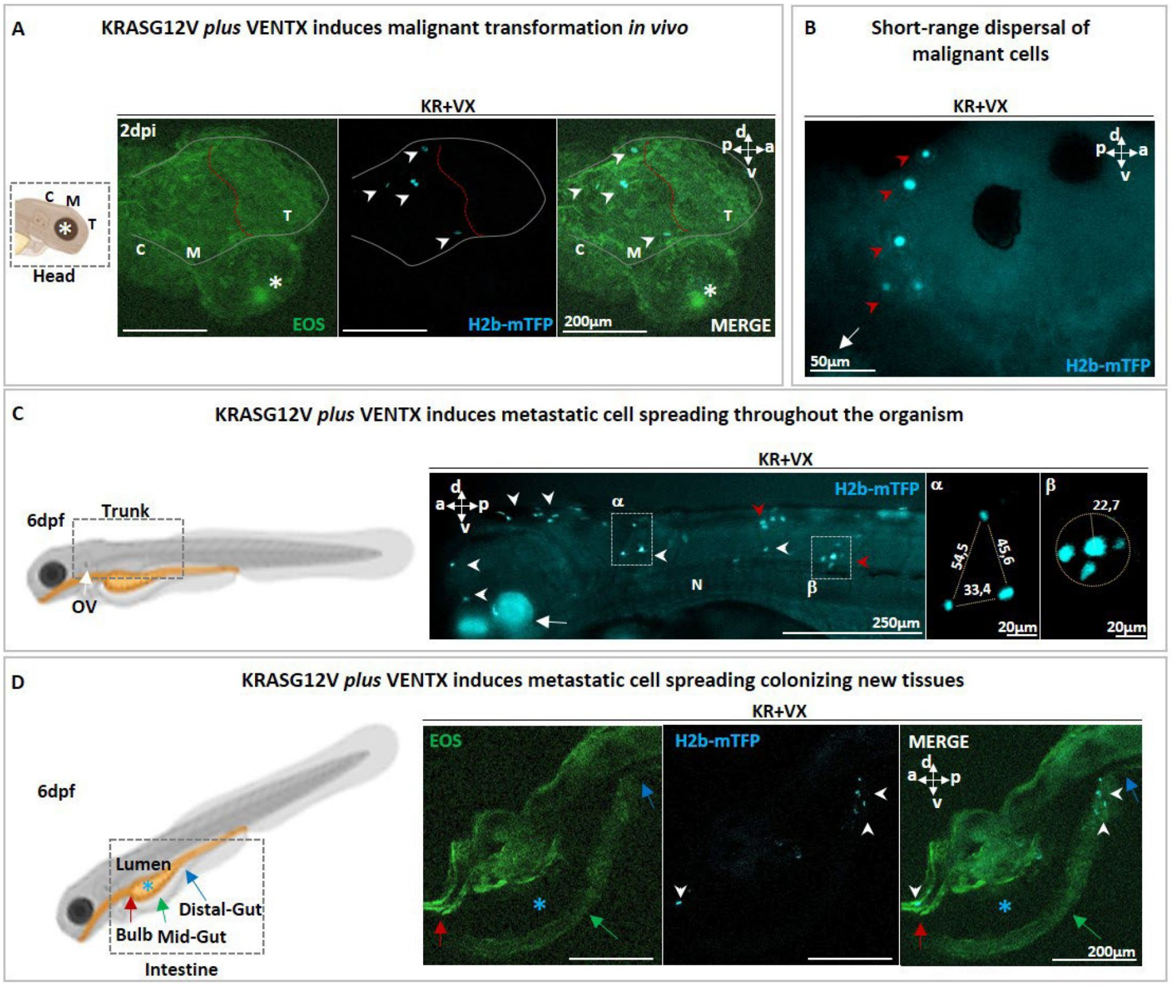

FIGURE S7

Metastatic spreading following activation of KRASG12V and Ventx (KR+VX).

(A) Schematic representation and confocal microscopy of zebrafish head showing the early malignant cells (H2B-mTFP $^{+}$ blue cells; white arrowheads) in the brain. Green EOS fluorescence has been used to visualize the whole zebrafish head. **(B)** Short range dispersal in the brain of the early progeny of the initial malignant cell (H2B-mTFP $^{+}$ blue cells; red arrowheads). An asterisk (*) indicate the eye and a white arrow the otic vesicle. **(C)** Schematic representation of the zebrafish larva trunk (left, dotted square), where H2B-mTFP^{+} cells (white arrowheads in center panel) can localize in KR+VX larvae, both as isolated cells (as in the dotted square α, 44,5µm of mean distance) or as small clusters (as in the dotted square β, r=22.7µm). **(D)** Schematic representation of zebrafish larva digestive tract (left, dotted square), and confocal microscopy showing H2b-mTFP^{+} cells (white arrowheads, center and right panel) localized in the gut. Green EOS fluorescence has been used to visualize the digestive tract. Red arrows indicate the bulb, the green arrows point to the mid-gut, the blue arrows the distal-gut and the blue asterisk (*) indicate to the gut lumen. Scale bars and body axes (a: anterior; p: posterior; d; dorsal; v: ventral) are shown.

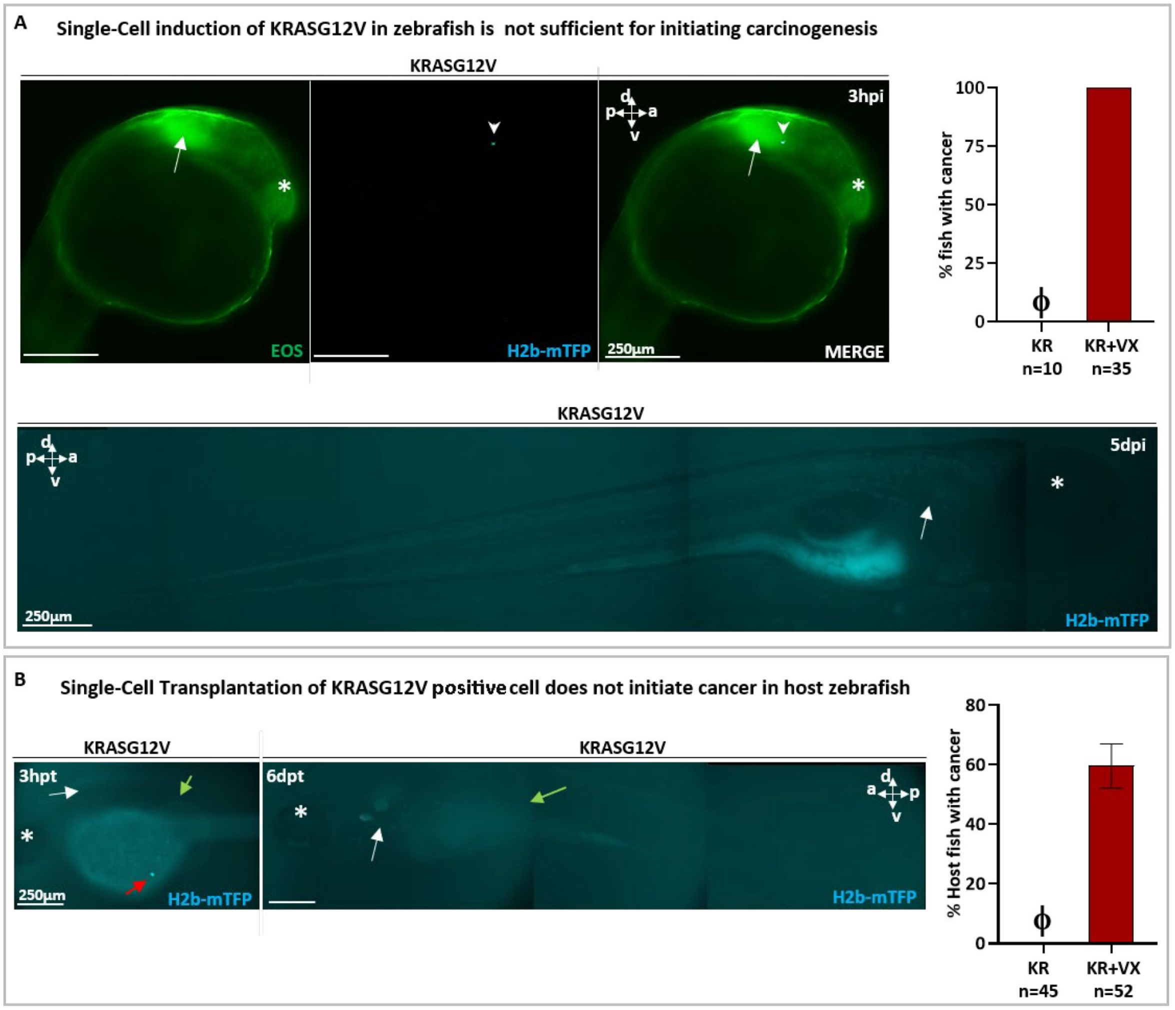

FIGURE S8

Single-cell activation of the KRASG12V oncogene is not sufficient to initiate carcinogenesis.

(A) At 1dpf, a single cell in the brain was photo-induced to express the oncogene kRasG12V and identified (white arrowhead) within ~30 min by the blue fluorescence of the expression marker (H2b-mTFP). The otic vesicle (indicated by white arrow) is used as a spatial reference. At 5 days post induction (5 dpi), the activated cell has disappeared. Note in the graph that, whereas KRASG12V *plus* VENTX (KR+VX) efficiently induces cancer (100%), KRASG12V alone (KR) is not sufficient (0%, indicated by φ). **(B)** Expression of kRasG12V was activated in 1 dpf embryos (without subsequent activation of Ventx). The cells of the larvae were dissociated and isolated cells (kRas expressing, H2b-mTFP^{+} blue cells) were transplanted (≈ 1 cell *per* host) at 2dpf in a *Nacre* (*mitf* -/-) zebrafish line for a better tracking of the transplanted cells. The transplanted H2b-mTFP^{+} blue cell (red arrow) can be visualized as early as 3 hours post transplantation (3hpt) in the yolk of the host. At 6 dpt the blue cell has disappeared in host *Nacre* zebrafish larvae. Note in the graph that, whereas the transplanted cell experiencing KRASG12V *plus* VENTX (KR+VX) activation efficiently give rise to cancer (60%), KRASG12V alone (KR) is not sufficient to initiate cancer in host zebrafish (0%, indicated by φ). In all figures, the otic vesicle (white arrow) is indicated as well as the eye (white asterisk: *). Scale bars and body axes (a: anterior; p: posterior; d; dorsal; v: ventral; l: left; r: right) are shown.

References

1 Cairns J. (1975) **Mutation selection and the natural history of cancer** *Nature* **255**:197–200

2 Riva L., et al. (2020) **The mutational signature profile of known and suspected human carcinogens in mice** *Nat. Genet* **52**:1189–1197

3 Adashek JJ, Kato S, Lippman SM, Kurzrock R. (2020) **The paradox of cancer genes in non-malignant conditions: implications for precision medicine** *Genome Med* **12**

4 Hanahan D., Weinberg R. A. (2000) **The hallmarks of cancer** *Cell* **100**:57–70

5 Soto A. M., Sonnenschein C. (2011) **The tissue organization field theory of cancer: a testable replacement for the somatic mutation theory** *BioEssays* **33**:332–340

6 Tomasetti C, Vogelstein B (2015) **Cancer etiology. Variation in cancer risk among tissues can be explained by the number of stem cell divisions** *Science* **347**:78–81

7 Jassim A, Rahrmann E.P, Simons B.D., Gilbertson R.J. (2023) **Cancers make their own luck: theories of cancer origins** *Nat.Rev.Can* **23**:710–724

8 Waclaw B., et al. (2015) **A spatial model predicts that dispersal and cell turnover limit intratumor heterogeneity** *Nature* **25**:261–264

9 Cairns J. (1975) **Mutation selection and the natural history of cancer** *Nature* **255**:197–200

10 Nowell P. C. (1976) **The clonal evolution of tumor cell populations** *Science* **194**:23–28

11 Hanahan D., Weinberg R. A. (2000) **The hallmarks of cancer** *Cell* **100**:57–70

12 Tomasetti C, Vogelstein B (2015) **Cancer etiology. Variation in cancer risk among tissues can be explained by the number of stem cell divisions** *Science* **347**:78–81

13 Frumkin D, et al. (2008) **Cell lineage analysis of a mouse tumor** *Cancer research* **68**:5924–5931

14 Malumbres M, Barbacid M. (2003) **RAS oncogenes: the first 30 years** *Nat Rev Cancer* **3**:459–465

15 Pylayeva-Gupta Y, Grabocka E, Bar-Sagi D (2011) **RAS oncogenes: weaving a tumorigenic web** *Nat Rev Cancer* **11**:761–74

16 Strachan T., Read A. P. (1999) **Chapter 18: Cancer Genetics** *Human molecular genetics*

17 Blasco MA (2005) **Telomeres and human disease: ageing, cancer and beyond** *Nat.Rev.Genet* **6**:611–622

18 Catalogue of Somatic Mutations in Cancer **Catalogue of Somatic Mutations in Cancer; https://cancer.sanger.ac.uk/cosmic**

19 Punekar SR, Velcheti V, Neel BG, Wong KK (2022) **The current state of the art and future trends in RAS-targeted cancer therapies** *Nat.Rev.Clin.Oncol* **19**:637–655

20 Merz V, et al. (2021) **Targeting KRAS: The Elephant in the Room of Epithelial Cancers** *Front.Oncol* **11**

21 Vogelstein B, Papadopoulos N, Velculescu VE, Zhou S, Diaz LA, Kinzler KW (2013) **Cancer genome landscapes** *Science* **339**:1546–58

22 Hepburn AC, et al. (2019) **The induction of core pluripotency master regulators in cancers defines poor clinical outcomes and treatment resistance** *Oncogene* **38**:4412–4424

23 Villodre ES, Kipper FC, Pereira MB, Lenz G. (2016) **Roles of OCT4 in tumorigenesis, cancer therapy resistance and prognosis** *Cancer Treat. Rev* **51**:1–9

24 Ducos B, Bensimon D, Scerbo P. (2022) **Vertebrate Cell Differentiation, Evolution, and Diseases: The Vertebrate-Specific Developmental Potential Guardians VENTX/NANOG and POU5/OCT4 Enter the Stage** *Cells* **11**

25 Rawat VP, et al. (2010) **The vent-like homeobox gene VENTX promotes human myeloid differentiation and is highly expressed in acute myeloid leukemia** *Proc Natl Acad Sci U S A* **107**:16946–51

26 Laise P, et al. **Developmental and MAPK-responsive transcription factors drive distinct malignant subtypes and genetic dependencies in pancreatic cancer**

27 Park Y, et al. (2021) **Transcriptomic Landscape of Lower Grade Glioma Based on Age-Related Non-Silent Somatic Mutations** *Curr. Oncol* **28**:2281–2295

28 Shibata H., et al. (2018) **In vivo reprogramming drives Kras-induced cancer development** *Nat.Comm* **9**

29 Adashek JJ, Kato S, Lippman SM, Kurzrock R. (2020) **The paradox of cancer genes in non-malignant conditions: implications for precision medicine** *Genome Med* **12**

30 Baggiolini A, et al. (2021) **Developmental chromatin programs determine oncogenic competence in melanoma** *Science* **373**

31 Ablain J, et al. (2018) **Human tumor genomics and zebrafish modelling identify SPRED1 loss as a driver of mucosal melanoma** *Science* **362**:1055–1060

32 Kaufman CK, et al. (2016) **A zebrafish melanoma model reveals emergence of neural crest identity during melanoma initiation** *Science* **351**

33 Feng Z *et al.* (2017) **Optical Control of Tumor Induction in the Zebrafish** *Sci.Rep* **7**

34 Sinha DK, et al. (2010) **Photoactivation of the CreERT2 recombinase for conditional site-specific recombina-tion with high spatio-temporal resolution** *Zebrafish* **7**:199–204

35 Zhang W, et al. (2018) **Control of protein activity and gene expression by cyclofen-OH uncaging** *ChemBioChem* **19**:1–8

36 Feil R., et al. (1996) **Ligand-activated site-specific recombination in mice** *Proc Natl Acad Sci U S A* **93**:10887–10890

37 Scerbo P, Monsoro-Burq AH (2020) **The vertebrate-specific VENTX/NANOG gene empowers neural crest with ectomesenchyme potential** *Sci Adv* **6**

38 Lam KHB, et al. (2022) **Topographic mapping of the glioblastoma proteome reveals a triple-axis model of intra-tumoral heterogeneity** *Nat Commun* **13**

39 Campbell NR (2021) **Cooperation between melanoma cell states promotes metastasis through heterotypic cluster formation** *Dev Cell* **56**:2808–2825

40 Martincorena I, Campbell PJ (2015) **Somatic mutation in cancer and normal cells** *Science* **349**:1483–9

41 Brash D.E. (2015) **Preprocancer** *Science* **349**:867–868

42 Fearon E. R., Vogelstein B. (1990) **A genetic model for colorectal tumorigenesis** *Cell* **61**:759–767

43 Berenblum I., Shubik P. (1949) **The persistence of latent tumor cells induced in the mouse's skin by a single application of 9, 10-dimethyl-1, 2-benzanthracene** *Br. J. Cancer* **3**:384–386

44 Brown S *et al.* (2017) **Correction of aberrant growth preserves tissue homeostasis** *Nature* **548**:334–337

45 Porazinski S, de Navascués J, Yako Y, Hill W, Jones MR, Maddison R, Fujita Y, Hogan C. (2016) **EphA2 Drives the Segregation of Ras-Transformed Epithelial Cells from Normal Neighbors** *Curr Biol* **26**:3220–3229

46 van Neerven SM, Vermeulen L. (2023) **Cell competition in development, homeostasis and cancer** *Nat Rev Mol Cell Biol* **24**:221–236

47 Visvader JE (2021) **Cells of origin in cancer** *Nature* **469**:314–22

48 Westerfield M. (2000) **The Zebrafish Book** *A Guide for The Laboratory Use of Zebrafish (Danio rerio)*

49 Kimmel C.B., Ballard W.W., Kimmel S.R., Ullmann B., Schilling T.F. (1995) **Stages of embryonic development of the zebrafish** *Dev. Dyn* **203**:253–310

50 Mosiman C., et al. (2011) **Ubiquitous transgene expression and Cre-based recombination driven by the ubiquitin promoter in zebrafish** *Development* **138**:169–177

51 Zhang W., Scerbo P., Delagrange M., Candat V., Mayr V., Vriz S., Distel M., Ducos B., Bensimon D. (2022) **Fgf8 dynamics and critical slowing down may account for the temperature independence of somitogenesis** *Commun.Biol* **5**

52 Bresciani E, Broadbridge E., Liu P.P. (2018) **An efficient dissociation protocol for generation of single cell suspension from zebrafish embryos and larvae** *MethodsX* **5**:1287–1290

Editors

Reviewing Editor

Filippo Del Bene

Institut de la Vision, Paris, France

Senior Editor
Richard White
University of Oxford, Oxford, United Kingdom

Reviewer #1 (Public Review):

Scerbo et al. developed an approach based on the oncogene kRasG12V and a reprogramming factor to induce deterministic and reproducible malignant transformation in a single cell. The activation of kRasG12V alone is not sufficient in their hands to initiate carcinogenesis, but when combined with the transient activation of a reprogramming factor (such as Ventx, Nanog, or Oct4), it significantly increases the probability of malignant transformation. This combination of oncogene and reprogramming factor may alter the epigenetic and functional state of the cell, leading to the development of tumors within a short period of time. The use of these two factors allows for the controlled manipulation of a single cell to study the cellular and molecular events involved in the early stages of tumorigenesis. The authors then performed allotransplantations of allegedly single fluorescent TICs in recipient larvae and found a large number of fluorescent cells in distant locations, claiming that these cells have all originated from the single transplanted TIC and migrated away. The number of fluorescent cells showed in the recipient larve just after two days is not compatible with a normal cell cycle length and more likely represents the progeny of more than one transplanted cell. The ability to migrate from the injection site should be documented by time-lapse microscopy. Then, the authors conclude that "By allowing for specific and reproducible single cell malignant transformation in vivo, their optogenetic approach opens the way for a quantitative study of the initial stages of cancer at the single cell level". However, the evidence for these claims are weak and further characterization should be performed to:

(1) show that they are actually activating the oncogene in a single cell (the magnification is too low and it is difficult to distinguish a single nucleus, labelling of the cell membrane may help to demonstrate that they are effectively activating the oncogene in, or transplanting, a single cell)
(2) the expression of the genes used as markers of tumorigenesis is performed in whole larvae, with only a few transformed cells in them. Changes should be confirmed in FACS sorted fluorescent cells
(3) the histology of the so called "tumor masses" is not showing malignant transformation, but at the most just hyperplasia. In the brain, the sections are not perfectly symmetrical and the increase of cellularity on one side of the optic tectum is compatible with this asymmetry.
(4) The number of fluorescent cells found dispersed in the larve transplanted with one single TIC after 48 hours will require a very fast cell cycle to generate over 50 cells. Do we have an idea of the cell cycle features of the transplanted TICs?

https://doi.org/10.7554/eLife.97650.1.sa2

Reviewer #2 (Public Review):

Summary:

In the work by Scerbo et al, the authors aim to better understand the open question of what factors constrain cells that are genetically predisposed to form cancer (e.g. those with a potentially cancer-causing mutation like activated Ras) to only infrequently undergo this malignant transformation, with a focus on the influence of embryonic or pluripotency factors (e.g. VENTX/NANOG). Using genetically defined zebrafish models, the authors can inducibly express the KRASG12V oncogene using a combination of Cre/Lox transgenes further controlled by optogenetically inducible Cre-activated (CreER fusion that becomes active with light-induced uncaging of a tamoxifen-analogue in a targeted region of the zebrafish embryo). They further show that transient expression and activation of a pluripotency factor (e.g. Ventx fused to a GR receptor that is activated with addition of dexamethasone) must occur in the model in order for overgrowth of cells to occur. This paper describes a genetically tractable and modifiable system for studying the requirements for inducing cellular hyperplasia in a whole organism by combining overexpression of canonical genetic drivers of cancer (like Ras) with epigenetic modifiers (like specific transcription factors), which could be used to study an array of combinations and temporal relationships of these cancer drivers/modifiers.

Strengths:

The combination of Cre/lox inducible gene expression with potentially localized optogenetic induction (CreER and uncaging of tamoxifen analogues) of recombination as well as well inducible activation of a transcription factor expressed via mRNA injection (GR-fusion to the TF and dex induction) offers a flexible system for manipulating cell growth, identity, and transcriptional programs. With this system, the authors establish that Ras activation and at least transient Ventx overexpression are together required to induce a hyperproliferative phenotype in zebrafish tissues.

The ability to live image embryos over the course of days with inducible fluorophores indicating recombination events and transgene overexpression offers a tractable in vivo system for studying hyperplastic cells in the context of a whole organism.

The transplant experiments demonstrate the ability of the induced hyperplastic cells to grow upon transfer to new host.

Weaknesses:

There is minimal quantitation of key aspects of the system, most critically in the efficiency of activation of the Ras-TFP fusion (Fig 1) in, purportedly, a single cell. The authors note "On average the oncogene is then activated in a single cell, identified within ~1h by the blue fluorescence of its nuclear marker) but no additional quantitative information is provided. For a system that is aimed at "a statistically relevant single-cell tracking and characterization of the early stages of tumorigenesis", such information seems essential.

The authors indicate that a single cell is "initiated" (Fig 2) using the laser optogenetic technique, but without definitive genetic lineage tracing, it is not possible to conclude that cells expressing TFP distant from the target site near the ear are daughter cells of the claimed single "initiated" cell. A plausible alternative explanation is 1) that the optogenetic targeting is more diffuse (i.e. some of the light of the appropriate wavelength hits other cells nearby due to reflection/diffraction), so these adjacent cells are additional independent "initiated" cells or 2) that the uncaged tamoxifen analogue can diffuse to nearby cells and allow for CreER activation and recombination. In Fig 2B, the claim is made that "the activated cell has divided, giving rise to two cells" - unless continuously imaged or genetically traced, this is unproven. In addition, it appears that Figures S3 and S4 are showing that hyperplasica can arise in many different tissues (including intestine, pancreas, and liver, S4C) with broad Ras + Ventx activation (while unclear from the text, it appears these embryos were broadly activated and were not "single cell activated using the set-up in Fig 1E? This should be clarified in the manuscript). In Fig S7 where single cell activation and potential metastasis is discussed, similar gut tissues have TFP+ cells that are called metastatic, but this seems consistent with the possibility that multiple independent sites of initiation are occurring even when focal activation is attempted.

Although the hyperplastic cells are transplantable (Fig 4), the use of the term "cells of origin of cancer" or metastatic cells should be viewed with care in the experiments showing TFP+ cells (Fig 1, 2, 3) in embryos with targeted activation for the reasons noted above.

https://doi.org/10.7554/eLife.97650.1.sa1

Reviewer #3 (Public Review):

Summary:

This study employs an optogenetics approach aimed at activating oncogene (KRASG12V) expression in a single somatic cell, with a focus on following the progression of activated cell to examine tumourigenesis probabilities under altered tissue environments. The research explores the role of stemness factors (VENTX/NANOG/OCT4) in facilitating oncogenic RAS (KRASG12V)-driven malignant transformations. Although the evidence provided are incomplete, the authors propose an important mechanism whereby reactivation of re-programming factors correlates with the increased likelihood of a mutant cell undergoing malignant transformation.

Strengths:

· Innovative Use of Optogenetics: The application of optogenetics for precise activation of KRAS in a single cell is valuable to the field of cancer biology, offering an opportunity to uncover insight into cellular responses to oncogenic mutations.
· Important Observations: The findings concerning stemness factors' role in promoting oncogenic transformation are important, contributing data to the field of cancer biology.

Weaknesses:

Lack of Methodological Clarity: The manuscript lacks detailed descriptions of methodologies, making it difficult to fully evaluate the experimental design and reproducibility, rendering incomplete evidence to support the conclusion. Improving methodological transparency and data presentation will crucially strengthen the paper's contributions to understanding the complex processes of tumourigenesis.
Sub-optimal Data Presentation and Quality:

The resolution of images throughout the manuscript are too low. Images presented in Figure 2 and Figure 4 are of very low resolution. It is very hard to distinguish individual cells and in which tissue they might reside.
Lack of quantitative data and control condition data obtained from images of higher magnification limits the ability to robustly support the conclusions.

Here are some details:
· Tissue specificity of the cells express KRASG12V oncogene: In this study, the ubiquitin promoter was used to drive oncogenic KRASG12V expression. Despite this, the authors claim to activate KRAS in a single brain cell based on their localized photo-activation strategy. However, upon reviewing the methods section, the description was provided that 'Localized uncaging was performed by illumination for 7 minutes on a Nikon Ti microscope equipped with a light source peaking at 405 nm, Figure 1. The size of the uncaging region was controlled by an iris that defines a circular illumination with a diameter of approximately 80 µm.' It is surprising that an epi-fluorescent microscope with an illumination diameter of around 80µm can induce activation in a single brain cell beneath skin tissue. Additionally, given that the half-life for mTFP maturation is around 60 minutes, it is likely that more cells from a variety of different lineages could be activated, but the fluorescence would not be visible until more than 1-hour post-illumination. Authors might want to provide more evidence to support their claim on the single cell KRAS activation.
· Stability of cCYC: The manuscript does not provide information on the half-life and stability of cCYC. Understanding these properties is crucial for evaluating the system's reliability and the likelihood of leakiness, which could significantly influence the study's outcomes.

· Metastatic Dissemination claim: Typically, metastatic cancer cells migrate to and proliferate within specific niches that are conducive to outgrowth, such as the caudal hematopoietic tissue (CHT) or liver. In figure 3 A, an image showing the presence of mTFP expressing cells in both the head and tail regions of the larva, with additional positive dots located at the fin fold. This is interpreted as "metastasis" by the authors. However, the absence of a supportive cellular compartment within the fin-fold tissue makes the presence of mTFP-positive metastatic cells there particularly puzzling. This distribution raises concerns about the spatial specificity of the optogenetic activation protocol.
The unexpected locations of these signals suggest potential ectopic activation of the KRAS oncogene, which could be occurring alongside or instead of targeted activation. This issue is critical as it could affect the interpretation of whether the observed mTFP signal expansion over time is due to actual cell proliferation and infiltration, or merely a result of ectopic RAS transgene activation.
· Image Resolution Concerns: The cells depicted in Figure 3C β, which appear to be near the surface of the yolk sac and not within the digestive system as suggested in the MS, underscore the necessity for higher-resolution imaging. Without clearer images, it is challenging to ascertain the exact locations and states of these cells, thus complicating the assessment of experimental results.
· The cell transplantation experiment is lacking protocol details: The manuscript does not adequately describe the experimental protocols used for cell transplantation, particularly concerning the origin and selection of cells used for injection into individual larvae. This omission makes it difficult to evaluate the reliability and reproducibility of the results. Such as the source of transplanted cells:
• If the cells are derived from hyperplastic growths in larvae where RAS and VX (presumably VENTX) were locally activated, the manuscript fails to mention any use of fluorescence-activated cell sorting (FACS) to enrich mTFP-positive cells. Such a method would be crucial for ensuring the specificity of the cells being studied and the validity of the results.
• If the cells are obtained from whole larvae with induced RAS + VX expression, it is notable and somewhat surprising that the larvae survived up to six days post-induction (6dpi) before cells were harvested for transplantation. This survival rate and the subsequent ability to obtain single cell suspensions raise questions about the heterogeneity of the RAS + VX expressing cells that transplanted.
· Unclear Experimental Conditions in Figure S3B: The images in Figure S3B lack crucial details about the experimental conditions. It is not specified whether the activation of KRAS was targeted to specific cells or involved whole-body exposure. This information is essential for interpreting the scope and implications of the results accurately.
· Contrasting Data in Figure S3C compared to literature: The graph in Figure S3C indicates that KRAS or KRAS + DEX induction did not result in any form of hyperplastic growth. This observation starkly contrasts with previous literature where oncogenic KRAS expression in zebrafish led to significant hyper-proliferation and abnormal growth, as evidenced by studies such as those published in and Neoplasia (2018), DOI: 10.1016/j.neo.2018.10.002; Molecular Cancer (2015), DOI: 10.1186/s12943-015-0288-2; Disease Models & Mechanisms (2014) DOI: 10.1242/dmm.007831. The lack of expected hyperplasia raises questions about the experimental setup or the specific conditions under which KRAS was expressed. The authors should provide detailed descriptions of the conditions under which the experiments were conducted in Figure S3B and clarifying the reasons for the discrepancies observed in Figure S3C are crucial. The authors should discuss potential reasons for the deviation from previous reports.

Further comments:

Throughout the study, KRAS-activated cell expansion and metastasis are two key phenotypes discussed that Ventx is promoting. However, the authors did not perform any experiments to directly show that KRAS+ cells proliferate only in Ventx-activated conditions. The authors also did not show any morphological features or time-lapse videos demonstrating that KRAS+ cells are motile, even though zebrafish is an excellent model for in vivo live imaging. This seems to be a missed opportunity for providing convincing evidence to support the authors' conclusions.

There were minimal experimental details provided for the qPCR data presented in the supplementary figures S5 and S6, therefore, it is hard to evaluate result obtained.

https://doi.org/10.7554/eLife.97650.1.sa0

Author response:

First we thank the reviewers for a thorough reading of our paper and some useful comments. A recurrent remark of the reviewers concerns the appearance of kRas-expressing cells (labelled by a nuclear blue fluorescent marker) which we attribute to the progeny of the initially induced cell. The reviewers suggest that these cells may have been obtained through activation of the Cre-recombinase in other cells by cyclofen released from light scattering, via diffusion, leakiness, etc. These remarks are perfectly reasonable from people not familiar with the cyclofen uncaging approach that we are using but are unwarranted as we shall show below.

We have been using cyclofen uncaging with subsequent activation of a Cre-recombinase (or some other proteins) since 2010 (see ref.34, Sinha et al., Zebrafish 7, 199-204 (2010) and our 2018 review (ref.35, Zhang et al., ChemBioChem 19,1-8 (2018)). In our experiments, the embryos are incubated in the dark in 6µM caged cyclofen (cCyc) and washed in E3 medium (or transferred to a new medium with no cCyc). In these conditions, over many years we never observed activation of the recombinase, i.e. the appearance of the associated fluorescent label in cells of embryos grown in E3 medium. Hence leakiness can be ruled out (in presence of cCyc or in its absence).

Following transfer of the embryos to new E3 medium we illuminate the embryos locally with light at 405nm. In these conditions, cCyc is only partially uncaged and results in activation of Cre-recombinase in only a few cells (1,2, 3, …) within the illuminated region only, namely in the appearance of the kRas-associated nuclear blue fluorescent label in usually one cell (and sometimes in a few more; data and statistics will be incorporated in a revised manuscript). In absence of any further treatment (e.g. activation of a reprogramming factor) these fluorescently labelled cells disappear within a few days (either via shut-down of their promotor, apoptosis or some other mechanism). The crucial point here is that we see less and not more kRas expressing cells (i.e. with nuclear blue fluorescence). This observation rules out activation of Cre-recombinase in other cells days after illumination due to leakiness, cyclofen released by light or diffusing from the illumination spot.

To observe many more fluorescent cells days after activation of the initial cell, one needs to transiently activate VentX-GR by overnight incubation in dexamethasone (DEX) (Injecting the embryos at 1-cell stage with VentX-GR or incubating them in DEX does not result in the appearance of more blue fluorescent cells). Following activation of VentX-GR, the fluorescent cells observed a couple of days after initiation are visualized in E3 medium (i.e. in absence of cyclofen) and are localized to the vicinity of the otic vesicle (the region where the initial cell was activated). In a revised manuscript we will present images of these fluorescent cells taken a few days apart from the same embryo in which a single cell was initially activated. Hence, we attribute these cells to the progeny of the activated cell. Obviously, single cell tracking via time-lapse microscopy would nail down this issue and provide fascinating insight into the initial stages of tumor growth. Unfortunately, immobilization of embryos in the usual medium (e.g. MS222, tricaine) over 5-6 days to track the division and motion of single cells is not possible. We are considering some other possibilities (immobilization in bungarotoxin or via photo-activation of anionic channels), but these challenging experiments are for a future paper.

> ***Reviewer #1 (Public Review):***
>
> *The authors then performed allotransplantations of allegedly single fluorescent TICs in recipient larvae and found a large number of fluorescent cells in distant locations, claiming that these cells have all originated from the single transplanted TIC and migrated away. The number of fluorescent cells showed in the recipient larve just after two days is not compatible with a normal cell cycle length and more likely represents the progeny of more than one transplanted cell.*

As mentioned in the manuscript, we measure the density of cells/nl and inject in the yolk of 2dpf Nacre embryos a volume containing about 1 cell, following published protocols (S.Nicoli and M.Presta, Nat.Prot. 2,2918 (2007)). We further image the injected cell(s) by fluorescence microscopy immediately following injection, as shown in Fig.4A and Fig.S8B. We might miss a few cells but not many. With a typical cell cycle of ~10h the images of tumors in larvae at 3dpt (and not 2dpt as misunderstood by this reviewer) correspond to ~100 cells. In any case the purpose of this experiment was not to study tumorigenesis upon transplantation but to show that the progeny of the initially induced cells is capable of developing into a tumor in a naïve fish, which is the operational definition of cancer that we adopted here.

> *The ability to migrate from the injection site should be documented by time-lapse microscopy.*

As stated above our purpose here is not to study tumor formation from transplanted cell(s) but to use that assay as an operational test of cancer. Besides as mentioned earlier single cell tracking in larvae over 3-4dpt is not a trivial task.

> *Then, the authors conclude that "By allowing for specific and reproducible single cell malignant transformation in vivo, their optogenetic approach opens the way for a quantitative study of the initial stages of cancer at the single cell level". However, the evidence for these claims are weak and further characterization should be performed to:*
>
> *(1) show that they are actually activating the oncogene in a single cell (the magnification is too low and it is difficult to distinguish a single nucleus, labelling of the cell membrane may help to demonstrate that they are effectively activating the oncogene in, or transplanting, a single cell)*

In a revised manuscript we will provide larger magnification of the initial induced cell and show examples of oncogene activation in more than one cell.

> *(2) the expression of the genes used as markers of tumorigenesis is performed in whole larvae, with only a few transformed cells in them. Changes should be confirmed in FACS sorted fluorescent cells*

When the oncogene is activated in a whole larvae all cells are fluorescent and thus FACS is of no use for cell sorting. Sorting could be done in larvae where single cells are activated, but then the efficiency of FACS is not good enough to isolate the few fluorescent cells among the many more non-fluorescent ones. We agree that the change in expression of the genes used as markers of tumorigenesis is an underestimate of their true change, but our goal at this time is not to precisely measure the change in expression level, but to show that the pattern of change is different from the controls and corresponds to what is expected in tumorigenesis.

> *(3) the histology of the so called "tumor masses" is not showing malignant transformation, but at the most just hyperplasia.*

The histology of the hyperplasic tissues displays cellular proliferation with a higher density of nuclear material which is characteristic of tumors, Fig.S4C. Besides the increased expression of pERK in these tissues, Fig.S4A,B is also a hallmark of cancer.

> *In the brain, the sections are not perfectly symmetrical and the increase of cellularity on one side of the optic tectum is compatible with this asymmetry.*

The expected T-shape formed by the sections of the tegmentum and hypothalamus are compatible with the symmetric sections shown in Fg.2D. The asymmetry in the optic tectum is a result of the hyperplasic growth.

> *(4) The number of fluorescent cells found dispersed in the larvae transplanted with one single TIC after 48 hours will require a very fast cell cycle to generate over 50 cells. Do we have an idea of the cell cycle features of the transplanted TICs?*

As answered above, the transplanted larvae are shown at 3dpt (and not 2dpt as misunderstood by this reviewer). With a cell cycle of about 10h, a single cell can give rise to about 100 cells in that time lapse.

> ***Reviewer #2 (Public Review):***
>
> *Summary:*
>
> *This paper describes a genetically tractable and modifiable system ...which could be used to study an array of combinations and temporal relationships of these cancer drivers/modifiers.*

We thank this referee for its positive comments. We would also like to point out that our approach provides for the first quantitative means to estimate the probability of tumorigenesis from a single cell, an estimate which is crucial in any assessment of cancer malignancy and the effectiveness of prophylactics.

> *Weaknesses:*
>
> *There is minimal quantitation of ... the efficiency of activation of the Ras-TFP fusion (Fig 1) in, purportedly, a single cell. ..., such information seems essential.*

In a revised manuscript we will add more images of induction of a single (or a few cells) and a table where the efficiency of RAS activation is detailed.

> *The authors indicate that a single cell is "initiated" (Fig 2) using the laser optogenetic technique, but without definitive genetic lineage tracing, it is not possible to conclude that cells expressing TFP distant from the target site near the ear are daughter cells of the claimed single "initiated" cell. A plausible alternative explanation is 1) that the optogenetic targeting is more diffuse (i.e. some of the light of the appropriate wavelength hits other cells nearby due to reflection/diffraction), so these adjacent cells are additional independent "initiated" cells or 2) that the uncaged tamoxifen analogue can diffuse to nearby cells and allow for CreER activation and recombination.*

We have addressed this point in our general comments to the reviewers’ remarks. The possibilities mentioned by this reviewer would result in cells expressing TFP in absence of

VentX activation, which is not the case. Cells expressing TFP away from the initial site are observed days after activation of the oncogene (and TFP) in a single cell and only upon activation of VentX.

> *In Fig 2B, the claim is made that "the activated cell has divided, giving rise to two cells" - unless continuously imaged or genetically traced, this is unproven.*

We have addressed this remark previously. Tracking of larvae over many days is not possible with the usual protocol using tricaine to immobilize the larvae. Nonetheless, in a revised version we will present images of an embryo imaged at various times post activation where proliferation of the cells can be observed. We are pursuing other alternatives for time-lapse microscopy over many days since, besides convincing the sceptics, a single cell tracking experiment (possibly coupled with in-situ spatial transcriptomics) will shed a new and fascinating light on the initial stages of tumor growth.

> *In addition, it appears that Figures S3 and S4 are showing that hyperplasia can arise in many different tissues (including intestine, pancreas, and liver, S4C) with broad Ras + Ventx activation .... This should be clarified in the manuscript).*

This is true and will be clarified in the new version.

> *In Fig S7 where single cell activation and potential metastasis is discussed, similar gut tissues have TFP+ cells that are called metastatic, but this seems consistent with the possibility that multiple independent sites of initiation are occurring even when focal activation is attempted.*

As mentioned previously this is ruled out by the fact that these cells are observed days after cyclofen uncaging (and TFP activation) and if and only if VentX is activated.

> *Although the hyperplastic cells are transplantable (Fig 4), the use of the term "cells of origin of cancer" or metastatic cells should be viewed with care in the experiments showing TFP+ cells (Fig 1, 2, 3) in embryos with targeted activation for the reasons noted above.*

The purpose of this transplantation experiment was to show that cell in which both kRas and VentX have been activated possess the capacity to metastasize and develop a tumor mass when transplanted in a naïve zebrafish. This - to the best of our knowledge - is the operational definition of a malignant tumor.

> ***Reviewer #3 (Public Review):***
>
> *Summary:*
>
> *This study employs an optogenetics approach ... to examine tumourigenesis probabilities under altered tissue environments.*

We thank this reviewer for this remark, since we believe that the opportunity to assess the probability of tumorigenesis from a single cell is possibly the most significant contribution of this work. To the best of our knowledge this has never been done before.

> *Weaknesses:*
>
> *Lack of Methodological Clarity: The manuscript lacks detailed descriptions of methodologies,*

In a revised manuscript we will include additional detail of our methodology.

> *Sub-optimal Data Presentation and Quality:*
>
> *Lack of quantitative data and control condition data obtained from images of higher magnification limits the ability to robustly support the conclusions.*

In a revised version we will include more images at higher magnification and quantitative data to support the main report of targeted single cell induction.

> *Here are some details:*
>
> *Authors might want to provide more evidence to support their claim on the single cell KRAS activation.*

More images and a data on activation of single or few cells in the illumination field will be provided in a revised version.

> *· Stability of cCYC: The manuscript does not provide information on the half-life and stability of cCYC. Understanding these properties is crucial for evaluating the system's reliability and the likelihood of leakiness, which could significantly influence the study's outcomes.*

We have been using the cCyc system for about 14 years. We refer the reader to our previous papers and reviews on this methodology (e.g. ref. 34,35). Briefly, cCyc is stable when not illuminated with light around 375nm. Typically, we incubate our embryos in the dark for about 1h before transferring them into E3 medium and illuminating them. Assessing the leakiness of the system is easy as expression of the fluorescent marker is permanently turned on. We have observed none in the conditions of our experiment.

> *· Metastatic Dissemination claim: However, the absence of a supportive cellular compartment within the fin-fold tissue makes the presence of mTFP-positive metastatic cells there particularly puzzling. This distribution raises concerns about the spatial specificity of the optogenetic activation protocol ... The unexpected locations of these signals suggest potential ectopic activation of the KRAS oncogene,*

We have addressed this remark in the introduction and above. Specifically, metastatic and proliferative mTFP-positive cells are observed if and only if VentX is also activated concomitant with activation of kRAS in a single cell. No proliferative cells are observed in absence of VentX activation, or in presence of VentX or Dex alone, or if kRAS has not been activated by cyclofen uncaging.

> *· Image Resolution Concerns: The cells depicted in Figure 3C β, which appear to be near the surface of the yolk sac and not within the digestive system as suggested in the MS, underscore the necessity for higher-resolution imaging. Without clearer images, it is challenging to ascertain the exact locations and states of these cells, thus complicating the assessment of experimental results.*

Better images will be provided in the revised version.

> *· The cell transplantation experiment is lacking protocol details:*

Details will be provided in the revised version. We have followed regular protocols for transplantation: S.Nicoli and M.Presta, Nat.Prot. 2,2918 (2007).

> • *If the cells are obtained from whole larvae with induced RAS + VX expression, it is notable and somewhat surprising that the larvae survived up to six days post-induction (6dpi) before cells were harvested for transplantation. This survival rate and the subsequent ability to obtain single cell suspensions raise questions about the heterogeneity of the RAS + VX expressing cells that transplanted.*

From Fig.S4D, about 50% of the embryos survive at 6dpi. Though an interesting question by itself we have not (yet) addressed the important issue of the heterogeneity of the outgrowth obtained from a single cell. Our purpose here was just to show that cells in which both kRAS and VentX have been activated possess the capacity to metastasize and develop a tumor mass when transplanted in a naïve zebrafish. This - to the best of our knowledge - is the operational definition of a malignant tumor.

> · *Unclear Experimental Conditions in Figure S3B: …It is not specified whether the activation of KRAS was targeted to specific cells or involved whole-body exposure.*

This was whole body (global) illumination and will be specified in the revised version.

> · *Contrasting Data in Figure S3C compared to literature: The graph in Figure S3C indicates that KRAS or KRAS + DEX induction did not result in any form of hyperplastic growth. The authors should provide detailed descriptions of the conditions under which the experiments were conducted in Figure S3B and clarifying the reasons for the discrepancies observed in Figure S3C are crucial. The authors should discuss potential reasons for the deviation from previous reports.*

This discrepancy will be discussed in the revised version. First the previous reports consider the development of tumors over a longer time-span (4-5 weeks) which we have not studied here. Second, the expression of the oncogene in these reports might be stronger than in ours. Third, the stochastic appearance of tumors in these reports suggest that some other mechanism (transient stress-induced reprogramming?) might have activated the oncogene in the initial cell.

Further comments:

> *Throughout the study, KRAS-activated cell expansion and metastasis are two key phenotypes discussed that Ventx is promoting. However, the authors did not perform any experiments to directly show that KRAS+ cells proliferate only in Ventx-activated conditions.*

Yes, we did. See Fig. S1 and compare with Fig.S3B, or Fig.S8A in comparison with Fig.2A,B.

> *The authors also did not show any morphological features or time-lapse videos demonstrating that KRAS+ cells are motile, even though zebrafish is an excellent model for in vivo live imaging. This seems to be a missed opportunity for providing convincing evidence to support the authors' conclusions.*

Performing single cell time-lapse microscopy on larvae over many (4-5) days is not possible with the regular tricaine protocol for immobilization. We are definitely planning such experiments, but they will require some other protocol, perhaps using bungarotoxin or some optogenetic inhibitory channels. Nonetheless, in the revised version we will show images of the same embryos at various times post single cell induction displaying proliferation of cells.

> *There were minimal experimental details provided for the qPCR data presented in the supplementary figures S5 and S6, therefore, it is hard to evaluate result obtained.*

More details will be given in the revised version.

https://doi.org/10.7554/eLife.97650.1.sa4